

VILNIUS UNIVERSITY

Sandra

BARONAITĖ

The studies of amniotic fluid and amniotic fluid stem cells

SUMMARY OF DOCTORAL DISSERTATION

Physical Sciences,

Biochemistry 04P

VILNIUS 2018

The study was conducted at Vilnius University Life Sciences Center Institute of Biochemistry (until 2016 Vilnius University, Institute of Biochemistry) from 2011 – 2017.

Academic supervisor:

Prof. dr. Rūta Navakauskienė (Vilnius University, Life Sciences Center, Institute of Biochemistry, Physical Science, Biochemistry – 04P)

Academic consultant:

Assoc. prof. dr. Audronė Arlauskienė (Vilnius University, Biomedical Sciences, Medicine – 06B)

This doctoral dissertation will be defended in a public/closed meeting of the Dissertation Defence Panel:

Chairman – Dr. Augustas Pivoriūnas (State Research Institute Centre for Innovative Medicine, Physical Sciences, Biochemistry – 04P)

Members:

Prof. dr. Diana Ramašauskaitė (Vilnius University, Biomedical Sciences, Medicine – 06B);

Prof. dr. Genė Biziulevičienė (State Research Institute Centre for Innovative Medicine, Biomedical Sciences, Biology – 01B)

Dr. Jonas Cicėnas (Vilnius University, Physical Sciences, Biochemistry – 04P)

Prof. dr. Gediminas Čepinskas (Lawson Health Research Institute and University of Western Ontario, Canada, Physical Sciences, Biochemistry – 04P)

The dissertation shall be defended at a public/closed meeting of the Dissertation Defence Panel at 3:00 p.m. on the 28th of November, 2018 at Vilnius University Life Science Center (auditorium R102)
Address: Saulėtekio av. 7, LT-10257, Vilnius, Lithuania.

Summary of doctor dissertation was distributed on the 29th of October, 2018.

Doctoral dissertation is available for review at the Library of Vilnius University website: www.vu.lt/lt/naujienos/ivykiu-kalendorius.

VILNIAUS UNIVERSITETAS

Sandra
BARONAITĖ

VAISIAUS VANDENŲ IR IŠ JŲ IŠSKIRTŲ KAMIENINIŲ LĄSTELIŲ TYRIMAI

DAKTARO DISERTACIJOS SANTRAUKA

Fiziniai mokslai,
Biochemija 04P

VILNIUS 2018

Disertacija rengta 2011 – 2017 metais Vilniaus universiteto Gyvybės mokslų centro Biochemijos institute (buvęs Vilniaus universiteto Biochemijos institutas)

Mokslinis vadovas:

prof. dr. Rūta Navakauskienė (Vilniaus universitetas, fiziniai mokslai, biochemija – 04P).

Mokslinis konsultantas:

doc. dr. Audronė Arlauskienė (Vilniaus universitetas, biomedicinos mokslai, medicina – 06B).

Gynimo taryba:

Pirmininkas – **Dr. Augustas Pivoriūnas** (Valstybinis mokslinių tyrimų institutas Inovatyvios medicinos centras, fiziniai mokslai, biochemija – 04 P)

Nariai:

Prof. dr. Diana Ramašauskaitė (Vilniaus universitetas, biomedicinos mokslai, medicina – 06B)

Prof. dr. Genė Biziulevičienė (Valstybinis mokslinių tyrimų institutas Inovatyvios medicinos centras, biomedicinos mokslai, biologija – 01B)

Dr. Jonas Cicėnas (Vilniaus universitetas, fiziniai mokslai, biochemija – 04 P)

Prof. dr. Gediminas Čepinskas (Lawson sveikatos tyrimų institutas ir Vakarų Ontario universitetas, Kanada, fiziniai mokslai, biochemija – 04P)

Disertacija ginama viešame Gynimo tarybos posėdyje 2018 m. lapkričio mėn. 28 d. 15 val. Vilniaus universiteto Gyvybės mokslų centro R102 auditorijoje. Adresas: Saulėtekio al. 7, LT-10257 Vilnius, Lietuva.

Disertaciją galima peržiūrėti VU bibliotekose ir VU interneto svetainėje adresu: <https://www.vu.lt/naujienos/ivykiu-kalendorius>

1. INTRODUCTION

With the rapid development of biotechnology, tissue engineering, gene therapy and cell therapy all counts are confronted with specific and individual medical tasks for treatments. Therefore, for several decades a lot of attention has been focused on stem cell research: ways of obtaining it, isolation, and adaptation to clinical applications. Human stem cells have unique properties: self-renewal and differentiation into different types of tissue cells, and therefore they are most widely used and used for scientific, clinical research or treatment: immune system, tissue regeneration, cartilage, genetically inherited diseases, etc. As known peripheral blood stem cells have been successfully applied to therapy for some time and are being further explored (Ivanovs et al., 2014). It is also known that stem cells can be successfully isolated from the adipose tissue, bone marrow, dental pulp and amniotic fluid, so researchers and clinicians aim to find the most easily accessible cell sources and treatable cells (Mohamed-Ahmed et al., 2018) and more "younger" and more naive, because the quality of the cells depends on the individual, his age for further medical purposes (Stolzing et al. 2008). Amniotic fluid (AF) for many years have been used only for prenatal genetic testing to assess the fetal condition, but the wider possibilities and benefits of AF have been noticed, especially for AF stem cells (AFSC), which are embryonic like and have more advantages because they are derived from non-embryos, are genetically stable, without somatic mutations, retain the potentials of differentiation that determines their use in regenerative medicine without causing ethical and moral problems (Prusa et al., 2003; Antonucci et al., 2011; Klemmt et al., 2011). The characteristics of AF cells are quite extensively investigated and described (Kim et al., 2007; Hamid et al., 2017), but not much in different fetus anamnesis. One of the most important properties is their ability to differentiate into the tissues of all three germplasm strains, and they do not have the tendency for spontaneous differentiation and do not form teratomas (De Coppi et al., 2007) and meet the full profile of multipotent stem cells.

The aim of the study - to perform proteomic analysis of amniotic fluid and amniotic fluid stem cells, to determine characteristics of amniotic fluid stem cells in fetus-affected and normal pregnancies and to evaluate the potential use of the research in the clinical practice.

Study objectives:

1. To determine the characteristics of stem cells isolated from fetus-affected and normal pregnancies amniotic fluid, to evaluate cell proliferation, aging and differentiation.
2. To identify the morphological, epigenetic and molecular changes in aging stem cell cultures.
3. To evaluate the profile of epigenetic modifications of stem cells of the normal and pathological pregnancies, depending on the phenotype and growth characteristics of the cells.
4. To identify specific proteins and their changes in the stem cells differentiated to adipogenic, osteogenic, myogenic and neurogenic lineages by performing detailed proteomic analysis.
5. To perform the proteomic analysis of amniotic fluid in normal and pathological pregnancies and determine the composition and differences of identified proteins.

Scientific novelty

The potential of stem cell is clear, but little detail and more extensive research has been done on fetal developmental pathologies. Collaboration with gynaecologists and geneticists of Vilnius University Hospital Santaros Klinikos provided the opportunity to receive biological material in various pregnancy conditions and to carry out protein analysis of amniotic fluid (AF), to determine the characteristics of isolated stem cells and to improve the cell isolation protocol with very small volumes of the biological material. The thesis presents the evaluation of stem cell proliferation features and differentiation possibilities, the proteomic profile of differentiated cells in different directions, identification of protein characteristics of amniotic fluid in different fetal anamnesis. The composition and differences of proteins found in AF and evaluates their potential biologic biomarkers, use in prenatal diagnostics.

Statements to be defended:

1. The immunogenic, stemness and proliferation properties of AF stem cells depends on individual itself, pregnancy trimester and the pathology of the fetus.
2. The aging AF stem cell cultures are characterized by morphological and epigenetic changes, and the expression of age-related protein markers (p16, p21, p53, ATM) and microRNA (miR-17, miR-21) depends on the intensity of the aging process.
3. Normal and pathological pregnancies AF stem cells are characterized by specific profile of chromatin activating and repressive histone modifications, depending on their phenotypic and growth characteristics.
4. AF stem cells can differentiate into myogenic, neurogenic, adipogenic, chondrogenic and osteogenic lineages with characteristic protein changes.
5. Amniotic fluid proteome composition depends on pregnancy status (normal vs. pathological).

2. MATERIALS AND METHODS

2.1. Isolation and Expansion of Mesenchymal Stem Cells from Amniotic Fluid

Samples (about 2-4 ml) were obtained by amniocentesis from mid second- (16–24 weeks) or third-trimester (28-38 weeks) including polyhydramnios cases using protocols approved by the Ethics Committee of Biomedical Researches of Vilnius District, number 158200-123-428-122 and maintained at room temperature up to 4 hours prior to isolation of amniotic cells using two stage protocol. The sample was centrifuged at 600 G (or 1,800 rpm) for 20 min, the supernatant was removed and the cell pellet was washed once with sterile PBS to remove blood and cell debris. After centrifugation, the cell pellet was resuspended in 5 ml of growth medium and plated in a 25 cm² culture flask.

2.2. Amniotic Fluid Stem Cells Isolation by Two Stage Protocol

Amniocytes were incubated for 5–15 days at 37°C in 5% CO₂, when first colonies appeared (first stage). For culturing of amniotic fluid mesenchymal stem cells (AF-MSCs), (-second stage), non-adhering AF cells were collected from primary culture and further expanded in a new 25 cm² culture flask at 37°C in 5% CO₂. After the appearance of cell colonies, the growing medium was changed every 3 days. When cells reached confluence at 80%, subculturing into higher passages was performed by trypsinization with 0.05% trypsin-EDTA for 3 minutes. Cells were subcultured by seeding (1x10⁴ cell/cm²). A morphologically homogeneous population of fibroblast-like cells was obtained after two rounds of subculture. Cell morphology was observed by phase-contrast microscope. Cell population doubling levels are presented as the average values calculated as follows: cell culture time (days)/number of passages. Cells were subcultured until they reached morphological changes related to senescence which was assessed using the β -galactosidase staining kit following the manufacturer's instruction. Stained cells were viewed under a phase-contrast microscope (Nikon Eclipse TS100) and the data was expressed as the percentage of β -galactosidase positive cells

2.3. Flow Cytometry Analysis

For identification of the phenotype of AF-MSCs from passages 4-5, cells were collected by centrifugation at 1,200 rpm for 6 min, washed once in phosphate buffered saline (PBS) with 0.2% fetal calf serum (FCS), and centrifuged again. A total of 5 · 10⁵ cells were resuspended in 50 μ L of PBS with 1% BSA and incubated with fluorescein isothiocyanate- (FITC-) conjugated mouse antihuman antibodies against CD44, CD34, CD90 or phycoerythrin- (PE-) labelled CD105, and appropriate isotype control mouse IgG2A-FITC or IgG1-PE. Samples were incubated in the dark at 4°C for 30 min and analysis was performed on a flow cytometer BD FACSCanto II with BD FACS Diva software.

2.4. RNA Isolation and RT-qPCR

MSCs from AF samples were cultured for 3–8 passages and analyzed for stem cell specific markers. Total RNA was extracted by TRIzol as recommended by the manufacturer, and then reverse-transcribed into cDNA using Maxima First Strand cDNA Synthesis Kit. qPCR was performed with Maxima SYBR Green qPCR Master Mix on the Rotor-Gene 6000 system. The amount of mRNA was normalized to GAPDH. The relative gene expression was calculated by a comparative threshold cycle delta-delta Ct method. Statistical analysis was performed using Student's *t*-test. Forward (F) and reverse (R) primers (5' - 3') used in RT-qPCR are as follows:

Adiponectin - F: GGAGACAGCTACTCCCCAAGAT; R:GTCCAGTCTTACCTCTCAAACCT
 ALP – F: AGCCCTTCACTGCCATCCTGT; R: ATTCTCTCGTTCACCGCCAC
 ATM: F: CTCTGAGTGGCAGCTGGAAGA; R: TTTAGGCTGGGATTGTTCGCT
 GAPDH - F: AACTCTGGTAAAGTGGATATTG; R: GGTGGAATCATATTGGAACA
 Myogenin - F: CAGCGAATGCAGCTCTCCACA; R: AGTTGGGCATGGTTCATCTG
 Nanog - F: CCTATGCCTGTGATTTGTGG; R: CCGGGACCTTGTCTTCCTTT
 Nestin - F: CAGCTGGCGCACCTCAAGATG; R: AGGGAAGTTGGGCTCAGGACTGG
 OCT-4 - F: CTCCTGGAGGGCCAGGAATC; R: CCACATCGGCCTGTGTATAT
 p16: F: GCTGCCCAACGCACCGAATA; R: ACCACCAGCGTGTCCAGGAA
 p21: F: GGCAGACCAGCATGACAGATT; R: GCGGATTAGGGCTTCCTCT
 p53: F: TAACAGTTCCTGCATGGGCGGC; R: AGGACAGGCACAAACACGCACC
 Rex1: F: GCCTTATGTGATGGCTATGTGT; R: ACCCCTTATGACGCATTCTATGT
 Sox-2 - F: GGCAGCTACAGCATGATGCAGGAC; R: CTGGTCATGGAGTTGTACTGCAGT

2.5. Preparation of Proteins and Western Blotting

AF-MSC were harvested by centrifugation (500G, 6 min) after trypsinization with 0.05% trypsin EDTA and washed twice in ice cold PBS, resuspended in 10 volumes of lysis solution (62.5 mM Tris, pH 6.8, 100 mM DTT and 2% SDS, 10% glycerol). Benzonase was added to give a final concentration of 2.5 units/ml. Cell lysate was prepared by homogenization through the needle No. 21 on ice and then centrifuged at 20,000G for 10 min, 4°C. The supernatants were immediately subjected to electrophoresis. Protein concentrations were measured using commercial RCDC protein assay. The lysates were separated on a 7–15% polyacrylamide gradient SDS-PAGE gel and then transferred to a PVDF membrane. The filters were incubated with the primary antibody according to the manufacturer’s recommendations and then with horseradish peroxidase-conjugated (HPR) secondary antibody at room temperature for 1 h. The bands were developed using enhanced chemiluminescence detection according to manufacturer’s instruction. For Western blotting, the following antibodies were used: DNMT1 and EZH2 were from Cell Signaling; H3K9me3 was from Upstate; H3K27me3 and BMI1 were from Millipore; ATM, ATM (phospho S1981), and GAPDH were from Abcam; goat anti-rabbit or rabbit anti-goat HPR (horseradish peroxidase) linked secondary antibodies were from Dako Cytomation A/S.

2.6. Gel Electrophoresis

The isolated proteins were fractionated by two dimensional gel electrophoresis (2DE). An Immobiline DryStrip Kit, pH range 3-10, and Exel Gel SDS, gradient 8- 18% was used for 2DE. It was carried out according to the manufacturer’s instructions. For protein visualization gels were stained with Coomassie Blue stain.

2.7. Filter-Aided Protein Sample Preparation

Samples were concentrated on Amicon ultra - 0.5 ml 30 kDa centrifugal filter unit and were denatured in 8 M urea, 100 mM DTT solution with continuous rotation at 800 rpm in the temperature controlled shaker for 3 hours at 37°C. Trypsin digestion was done. Briefly, samples were washed with buffer containing 8

M urea. The proteins were alkylated using iodoacetamide. Buffer was exchanged by washing two times with 50 mM NH_4HCO_3 and proteins digested overnight with TPCK Trypsin 20233. After overnight digestion, peptides were recovered by centrifugation and then two additional washes using 50% CH_3CN were combined, acidified, lyophilized, redissolved in 0.1% formic acid, and then analyzed by mass spectrometry.

2.8. Liquid Chromatography and Mass Spectrometry

Liquid chromatography and mass spectrometry were performed as described earlier (Savickiene et al., 2015). The samples were run in triplicate.

2.9. Data Processing, Searching, and Analysis

Raw data files were processed and searched using ProteinLynx Global SERVER (PLGS). The identified proteins were analyzed for their functional properties by using UniprotKB/SwissProt human database. The bioinformatics pipeline ISOQuant (<http://www.immunologie.uni-mainz.de/isoquant/>) was used for label-free quantification. t-tests were performed on data to evaluate the difference between groups (MarkerView software, AB Sciex).

2.10. Differentiation Assays

AF-MSCs differentiation capacity was performed in a monolayer as detailed by manufacturer's protocol using commercially available STEM Pro Differentiation kits (Gibco, Invitrogen cell culture). AF-MSC were cultured at 80%–90% confluence and subsequently differentiated with STEMPro Differentiation medium at 37°C in 5% CO_2 . For cell staining, AF-MSCs were seeded into a 4-well (3.85 cm^2) plate (Nunc, Thermo Scientific, Roskilde, Denmark) at a 1×10^4 cells/ cm^2 . Each cell population was differentiated in 3 replicates using undifferentiated cells for controls. During cell differentiation, the medium was replaced every 2-3 days. For gene expression studies, AF-MSCs were cultured in a T-25 flask.

2.10.1. Adipogenic Differentiation

For adipogenic differentiation, AF-MSCs were cultured at 80% confluence and subsequently differentiated with STEM Pro Adipogenic Differentiation medium for 14–18 days at 37°C in 5% CO_2 . After specific period of cultivation, formation of intracellular lipid droplets was monitored by Oil Red O staining. In brief, cells were washed with 60% isopropanol, dried, and stained for 10 min in Oil Red O solution freshly diluted into distilled water at a ratio of 3:2, followed by three washes in distilled water. Adiponectin expression was determined by RT-qPCR.

2.10.2. Osteogenic Differentiation

For osteogenic differentiation, AF-MSCs after seeding at a 1×10^4 cells/ cm^2 into a 4-well plate or T-25 flask were cultivated in STEMPro Osteogenic Differentiation medium for 14–18 days at 37°C in 5% CO_2 , according to the manufacturer's instructions. Osteogenic differentiation was determined by alizarin red staining of the calcified extracellular matrix deposition. In brief, samples were fixed with 4% formaldehyde for 15 min at room temperature, washed twice with PBS, pH 4.2, and stained with 2% Alizarin Red in deionised water for 20 min at 37°C, followed by two washes in PBS. Osteopontin expression was determined by RT-qPCR.

2.10.3. Chondrogenic Differentiation

For chondrogenic differentiation, micromass cultures were generated by seeding 20 μL droplets of cells (1.6×10^4 cells/ μL in growing medium) into individual wells of 4-well plate. Cells were allowed to attach for 4 h at 37°C in 5% CO_2 under high humidity conditions before adding STEMPro Chondrogenic Differentiation medium for 14–18 days. Chondrogenic pellets were determined by staining for 30 min. with 1% alcian blue in 3% acetic acid, followed by three washes in 3% acetic acid and finally in water.

2.10.4. Myogenic Differentiation

For myogenic differentiation, cells were plated at a 1×10^4 cells/ cm^2 and cultured at 80% confluence and then washed with PBS before the incubation in DMEM containing antibiotics and 2% of horse serum (Invitrogen) for 14–18 days with low serum media changes every 2-3 days. Multinucleated cells were visualized by phase contrast microscope (Nikon Eclipse TS100) after staining with 0.1% crystal violet in 20% ethanol, followed by washing in water. Myogenin expression was determined by RT-qPCR.

2.10.5. Neural Differentiation

For neural differentiation, the induction medium containing 1 mM all-trans-retinoic acid (Sigma) in DMEM/F12 with GlutaMax and N2 supplement (Gibco, Life Technologies, Grand Island, NY, USA) was used after culturing cells at 60% confluence. A morphologic change to neuron-like cells with axonal outgrowth was visualized by phase contrast microscope after staining with 0.1% crystal violet. Nestin expression was determined by RT-qPCR.

2.11. Immunofluorescence Analysis

Cells were grown in multi-well tissue culture plates on cover glass. Samples were rinsed three times in PBS, pH 7.6, and fixed for 15 minutes with PBS supplemented with 4% (w/v) paraformaldehyde. After washing three times in PBS, cells were permeabilized with 0.2% Triton X-100 for 20 min, rinsed again and blocked for 30 min in PBS containing 1% BSA and 10% (v/v) goat serum (Dako Cytomation) at room temperature, washed with PBS/1% BSA and incubated with the indicated primary antibody against H4ac (penta), H4K16ac, H3K9ac, H3K14ac, H3K9me2, H3K9me3 (Upstate Biotechnology), H3K27me3 (Millipore), and 5-mC (Abcam) for 60 min at 37°C. Then cover slips were washed as before and incubated with the secondary antibody (Alexa Fluor 488, goat anti-rabbit IgG (H β L) for 60 min at 37°C in the dark. The same samples were incubated with DAPI for 10 min at room temperature. Immunostaining was repeated in three replicates and in more than three independent trials for each histone modification. The observed samples contained 70–80% of cells with a positive mark of the modified histone. Stained samples were washed and images were captured with Zen 2011 software program using Axio Cam HRm camera mounted on Carl Zeiss Overall View Axio Observer and Z1 microscope using 63X oil immersion objective with PBS supplemented with 4% (w/v) paraformaldehyde. After washing three times in PBS, cells were permeabilized with 0.2% Triton X-100 for 20 min, rinsed again and blocked for 30 min in PBS containing 1% BSA and 10% (v/v) goat serum (Dako Cytomation) at room temperature, washed with PBS/1% BSA and incubated with the indicated primary antibody against H4ac (penta), H4K16ac, H3K9ac, H3K14ac, H3K9me2, H3K9me3 (Upstate Biotechnology), H3K27me3 (Millipore), and 5-mC (Abcam) for 60 min at 37°C. Then cover slips were washed as before and incubated with the secondary antibody (Alexa Fluor 488, goat anti-rabbit IgG (H + L) for 60 min at 37°C in the dark. The same samples were incubated with DAPI for 10 minutes at room temperature. Immunostaining was repeated in three replicates and in more than three independent trials for each histone modification. The observed samples contained 70–80% of cells with a positive mark of the

modified histone. Stained samples were washed and images were captured with Zen 2011 software program using Axio Cam HRm camera mounted on Carl Zeiss Overall View Axio Observer and Z1 microscope using 63X oil immersion objective. Custom image processing and analysis tools were employed to evaluate changes of integrated fluorescence intensities (IFIs) in areas of interest (nuclei regions). Required tools have been implemented in Matlab™ environment (The MathWorks, Natick MA). To obtain integrated intensities, it was necessary to segment DAPI images (find borders of nuclei) and sum up intensity values of Alexa Fluor 488 image pixels that belong to nuclei regions. Image segmentation to acquire nuclei regions includes image manipulation steps like Gaussian image smoothing for noise reduction, symmetrical feature detection, Watershed transformation and thresholding. Other minor processing steps were used to ensure solidity of nuclei regions. Symmetrical feature detector generates map of second order symmetries using Johansson method (Johansson, 2004). Watershed transformation partitions symmetry maps into distinct regions and simple thresholding determines area of nuclei inside watershed regions. Protein quantity in the particular area of the cell is related to IFI in a segmented region of the corresponding cell. Previously detected nuclear areas in DAPI images were used as regions of interest (ROIs) for calculations of IFIs, where (x, y) represents pixel coordinates.

$$IFI = \sum_{(x,y) \in ROI} I^{FITC}(x,y)$$

2.12. Statistical Analysis

All values of flow cytometry, RT-qPCR, and Western blot analysis are expressed as mean \pm SD. Student's paired t test was performed for comparison of data of paired samples, the values *P < 0.05, ** P < 0.01, and *** P < 0.001 were considered statistically significant.

3. RESULTS

3.1. Characterization of MSC Population from Amniotic Fluid of Late Second- and Third-Trimester

3.1.1. Cell Morphology

Amniotic fluid cells represent a heterogeneous population and 1% demonstrates stem cell characteristics. In our study we used a two-step cultivation protocol to isolate stem cells. Adherent cells derived from fresh AF samples in primary culture resulted in a mixed population with spindle round-shaped morphology forming colonies at about 7–20 days of culture (fig. 1A). The colonies of small and spherical cells with a centrally located nucleus resemble epithelial cells that form islands in culture of 2-3 passages (fig. 1B). The primary culture contained a slowly growing cell population, which displayed large and flat “stromal” cells with irregular cytoplasmic extensions and very small nucleus at the edge of cytoplasm (fig. 1D). Cells of fibroblast-like morphology with a high proliferation potential were present in culture after the second and third passage as well (fig. 1C). The derivation of mesenchymal stem cell population using two-step protocol was successful, and after 4–8 passages in culture, the population became morphologically homogeneous with fibroblastic morphology (fig. 1C and 2A). These AF-MSCs grew to 80–90% confluence of the subsequent passage culture in 2–4 days and were tested on their cellular phenotypic characteristics and differentiation potential at passages 4–6.

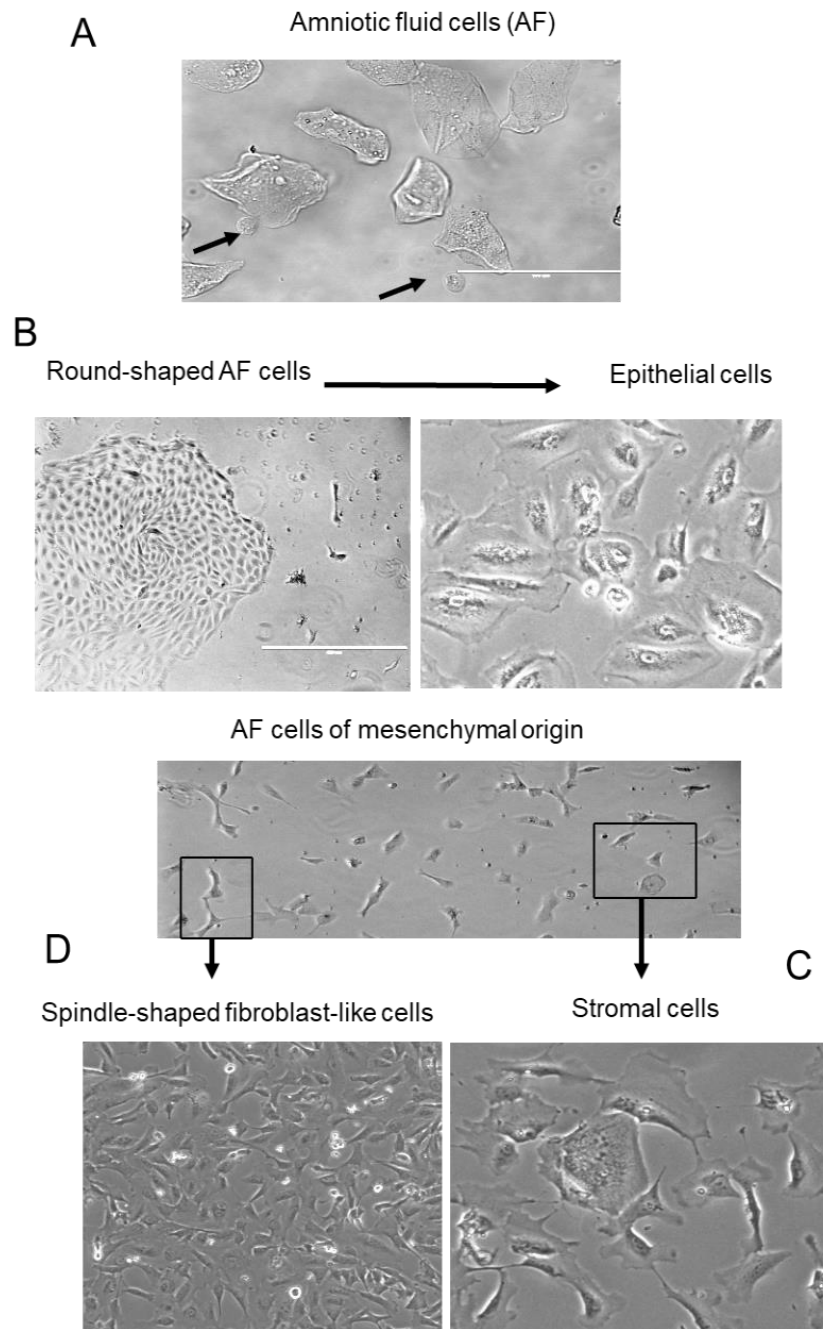


Figure 1. Morphological characteristics of AF cells. (A) Amniotic fluid cells. (B) The colony appearance of epithelial type at 7–20 days after initiation of the primary culture at passage 3. (C, D) Mesenchymal-type cells in the primary culture at 10–15 days and after culturing to elongated spindle-shaped and/or flat “stromal” cell populations at passage 3.

3.1.2. AF-MSCs Immunophenotypic Characteristics

MSCs from AF amniocentesis samples from normal pregnancies (group N) were successfully isolated and cultivated. Amniotic fluid cell cultures observation and their morphologic, phenotypic, and growth

characteristics from normal pregnancies at 16–20 week of gestation were performed. Cells formed and maintained homogeneous populations with predominant mesenchymal-type cells of spindle-shaped morphology during passaging (fig. 2A). MSCs cultures mesenchymal cell origin in AF samples was evaluated by the presence of the cell surface markers monitored by flow cytometry at passage 5. The representative histograms of MSCs from AF of healthy pregnancies gated for cell surface markers prior to analysis of the isotype-matched negative controls and are shown in Fig. 2B. The positive expression of cell surface pluripotency markers, CD105 (78.4±3.8%) and CD44 (89.7±3.4%), and the mesenchymal marker CD90 (92.7±2.8%) was detected in all samples with predominant mesenchymal-type morphology. The hematopoietic marker CD34 was absent in all AF-MSCs populations. To confirm stem cell origin, we performed RT-qPCR analysis of transcription factors Oct4, Nanog, Sox2, and Rex1 that are responsible for maintenance of multi-potency and self-renewal of MSCs. The data presented in Fig. 2C indicated quite similar expression levels of stemness markers in MSCs samples derived from AF of three individual normal pregnancies.

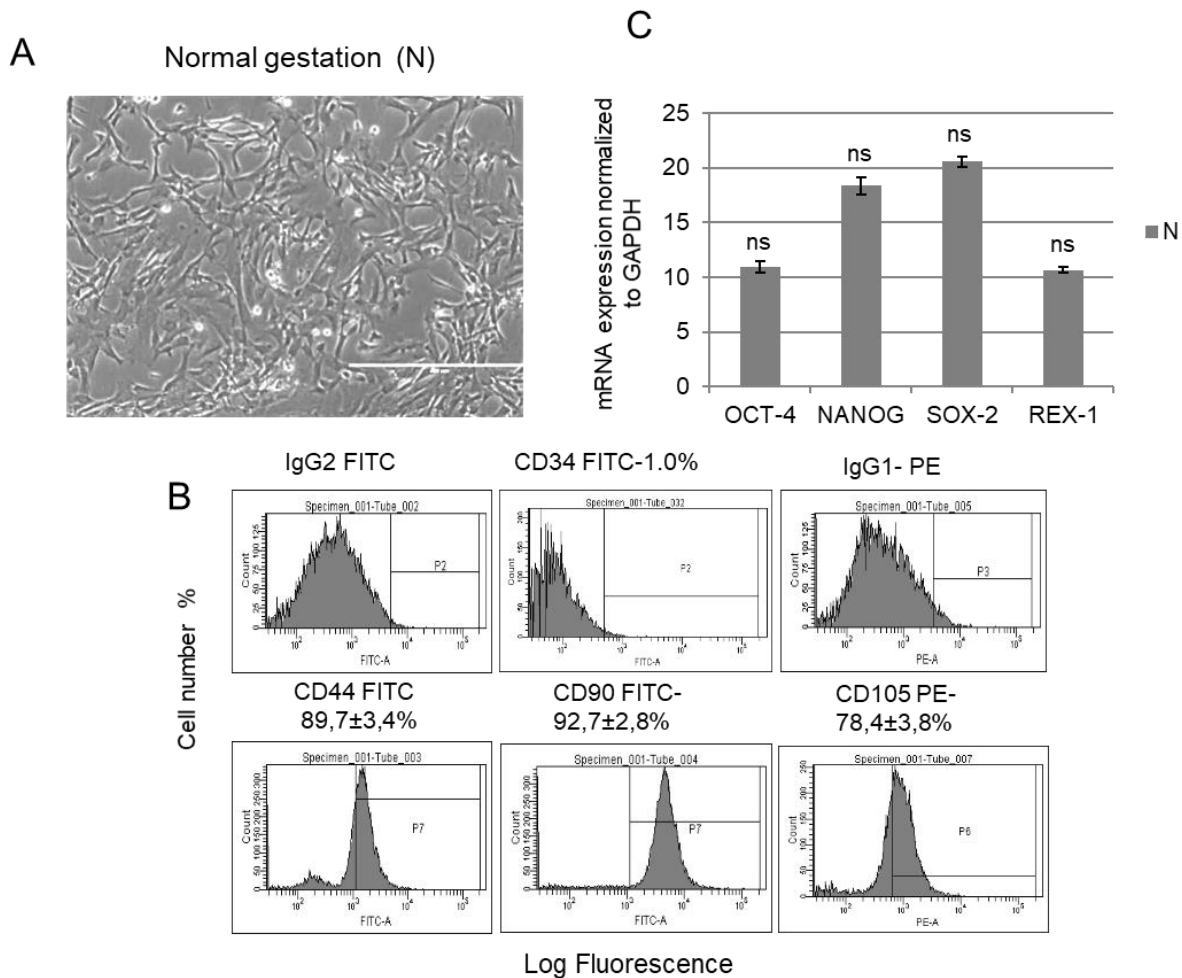


Figure 2. Characteristics of AF-MSCs derived from normal pregnancies. (A) Representative images of cell morphology. (B) Representative flow cytometry histograms of MSCs cultures from AF of normal gestations at passage 5. The values are expressed as the percentage of CD-positive cells. (C) The expression of stemness markers in (N) cultures at passage 5 determined by RT-qPCR and normalized to GAPDH expression levels. All data are presented as the mean ±SD, *P≤0.05 was considered as significant changes, ns non-significant changes.

3.1.3. AFMSC Stemness Markers

AF-MSCs of different gestation age (16-34 weeks) were evaluated for the expression of stem cell pluripotency markers and were responsible for maintenance of multi-potency and self-renewal of MSCs. Our results of RT-qPCR analysis demonstrated that MSCs at 4-6 passages consistently expressed: Oct-4, Sox-2, Nanog, Rex-1 (fig. 3B). AF-MSCs from second- and third- trimester (16-28 weeks) expressed comparable levels of Oct-4 and Nanog, while some difference in the expression levels of Sox-2 and Rex-1 was related to the gestational age. MSCs from third trimester of gestation (at 34 week) exhibited lower expression of Sox-2 and Rex-1 (fig. 3B).

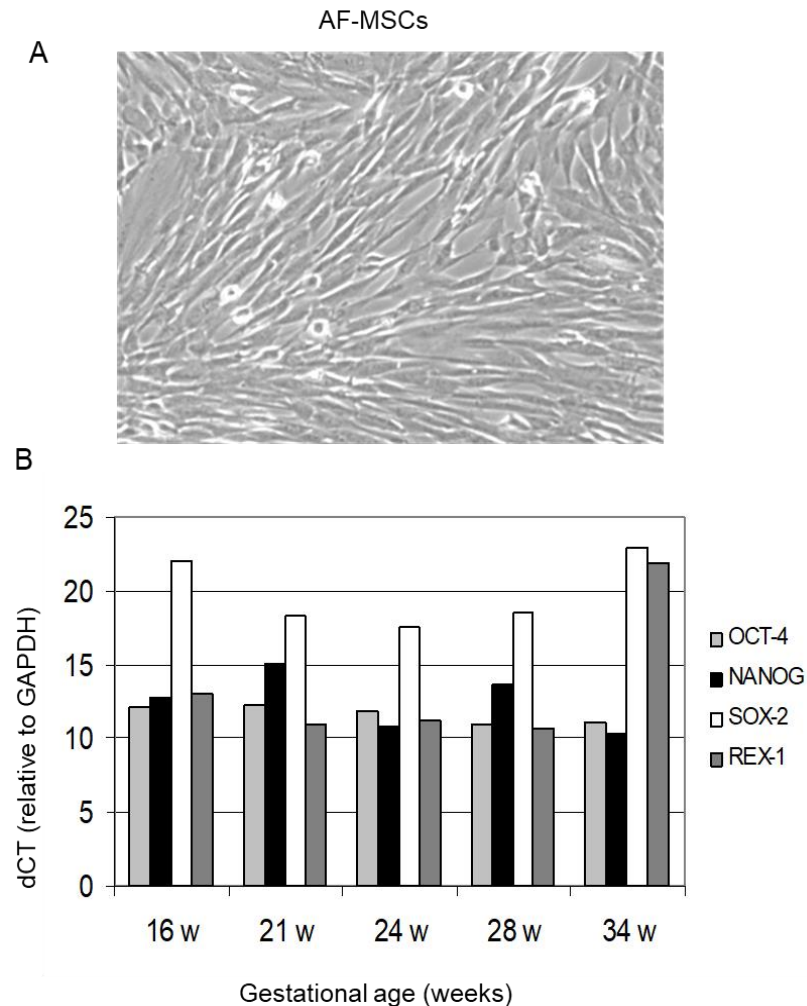


Figure 3. Phenotypical characteristics of AF-MSCs from third trimester. (A) Representative image of MSCs at passage 4. (B) The relative expression of pluripotency markers Oct4, Nanog, Sox2 and Rex1 in AF-MSCs populations obtained from amniocentesis samples of second- and third-trimester at passages 4-6 by RT-qPCR. The expression of mRNA was normalized to GAPDH.

3.2. Characterization of MSCs Cultures of Normal and Fetus-Affected Gestations

MSCs from amniocentesis samples of normal pregnancies (N) and pregnancies with fetus abnormalities were isolated and cultivated until the cells showed signs of decreased proliferation. We designated three groups of AF-MSCs cultures as N (n=3) from normal pregnancies at 16-20 week of gestation, PI (n=3) – AF samples from pregnancies with fetus structural abnormalities and group PII (n=3) – AF-MSCs derived from samples with fetal chromosomal changes. Adherent cells derived from fresh AF samples of late second-and third-trimester in primary culture resulted in a mixed population with spindle and round-shaped morphology forming colonies at about 15–20 days of culture. We were passaging cultures up to passages 8. MSCs cultures of N and P I group had quite similar characteristics that were distinct in samples of PII group at passage 5 (fig. 4A). Samples of PII group displayed lower proliferation levels and mesenchymal-type morphology with a variable portion of flattened cells appearing at passage 5 (fig. 4A). Such populations contained enlarged and flattened morphology with increased cytoplasmic granularity. The cell surface markers analysis of PI and PII cultures at passage 5 was performed by flow cytometry. As demonstrate representative histograms of sample from P I group (fig. 4B), MSCs maintained the original CD90 and CD105 expression profile but with less portion of CD44 positive cells compared with samples of N group (fig. 2B, 4B), in contrast to slower growing cells of sample from PII group showing a decline of CD90 (67.5%) marker and notably lower levels of CD44 (38.9%) and CD105 (31.3%) (fig. 4B). As it is shown, flow cytometry results did not present significant differences between MSCs cultures from N and P I group, while CD percentages were lower in all samples from P II group compared with others (fig. 2B, 4B).

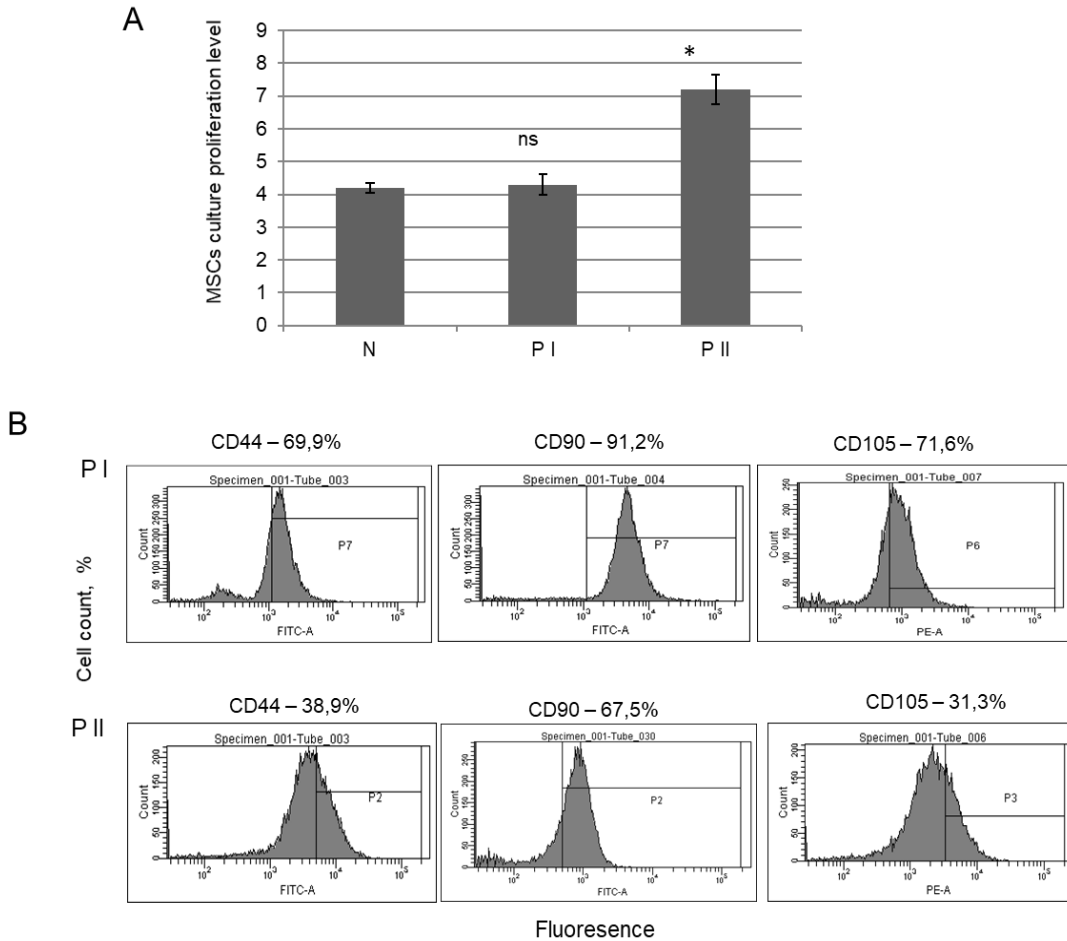


Figure 4. Characteristics of MSCs derived from AF of fetus-affected gestations. (A) The proliferation level (culturing time (days)/number of passages) of MSCs cultures derived from AF of normal gestation (N, n=3) and those with fetal abnormalities (P I and P II, n=3 in each group) during cultivation; P II cultures displayed relatively lower proliferation than N cultures. (B) Flow cytometry histograms of MSCs cultures from PI group and PII group at passage 5. The percentage mean of CD44, CD90 and CD105-positive cells in MSCs cultures from fetus-affected gestation at passage 5. All data are presented as the mean \pm SD, * $P \leq 0.05$ was considered as significant changes, ns - non-significant changes.

RT-qPCR analysis of stemness markers: Sox2, Oct4, Nanog, and Rex1 revealed their variable expression in groups PI and PII cultures. The comparison of stemness markers profile within groups indicated differences of Oct4 and Nanog expression, with relatively similar their expression in cultures from PI group but lower levels in PII group. Sox2 and Rex1 exhibited less expression variations in all cultures. The results indicate that cell surface and stemness markers profile is related to AF-MSCs state during cultivation or individual factors. We analyzed MSCs samples from normal and pregnancies with fetus abnormalities. Cell cultures were cultured for 3–9 consecutive passages and at each passage MSCs were replated at 80–90% confluence. At early passages (p3-4), cell cultures from both AF sources formed and maintained homogeneous populations of typical elongated mesenchymal-type and spindle-shaped morphology (fig. 5A). After passages 5-6 there was a decline in the efficiency of proliferation in all cell populations. Time to reach senescence differed between cultures. As shown (fig. 5B), some samples, including AF of normal pregnancies and with fetus effected gestation stopped proliferate earlier (at p5-6),

while others, slower proliferating cultures of fetus-pathological gestation, took longer time to achieve senescence (at p7-8). Morphological changes of cells were observed during passaging, where AF-MSCs cultures from different samples presented a typical MSCs morphology with the appearance of a varied proportion of flattened cells (fig. 5A). The comparison of images of cell cultures during passaging showed enlarged and flattened morphology cells with increased cytoplasmic granularity and frequency for positive staining with senescence associated β -galactosidase (SA- β -gal) at late passages (fig. 5C). These senescence-associated changes occurred later in AF-MSCs samples that showed relatively lower level of proliferation.

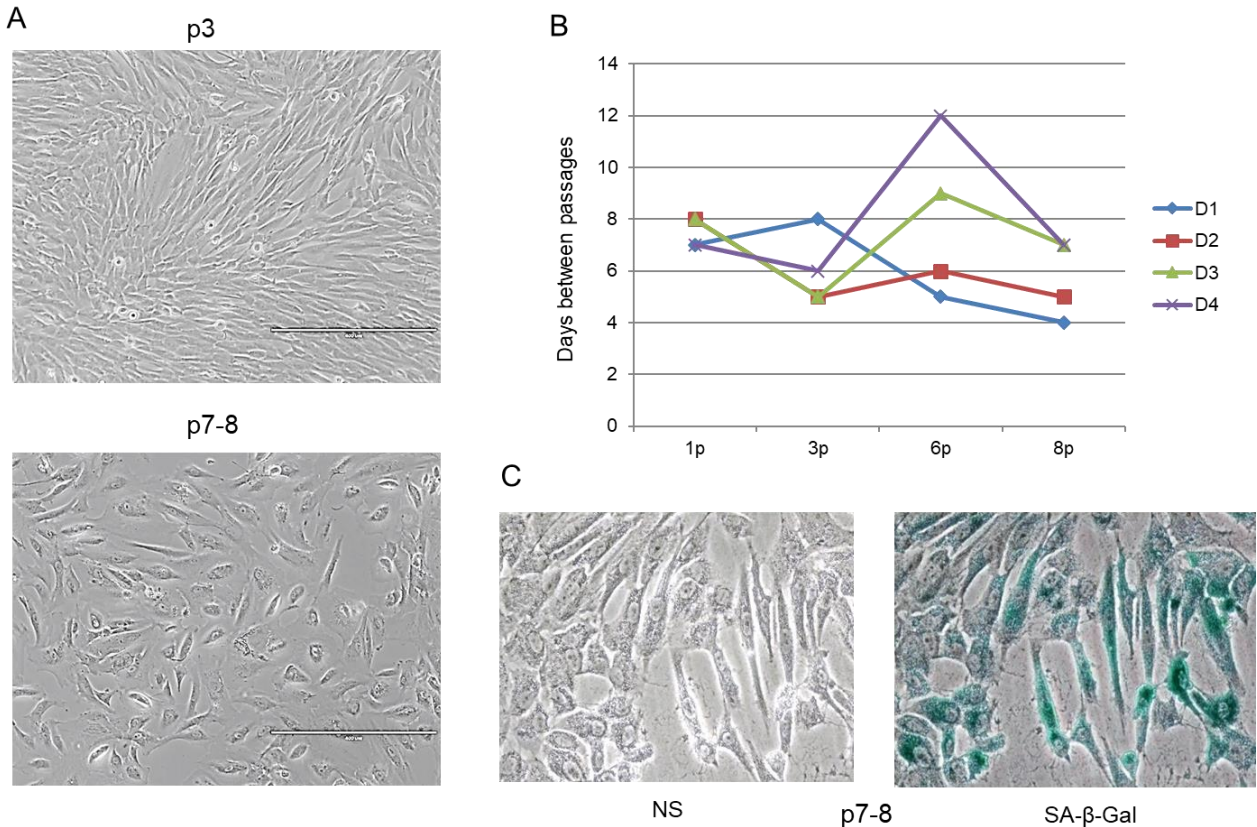


Figure 5. Characteristics of MSCs derived from AF of normal vs pathological gestation during cultivation. (A) Representative images of initially spindle-shaped MSCs morphology in early (p3) and senescent passages (p7-8). (B) Differential proliferation of MSCs from AF of individual donors (D) during cultivation to passage 8. (C) Senescence-associated β -galactosidase staining in the late passage (p7-8); NS-non stained cells.

3.3. Senescence-Associated Molecular Changes in MSCs Cultures

During passaging of MCS from two sample groups (I and II) of cell cultures, MSCs maintained their characteristic features as stemness factors, immunophenotype, but the proliferation potential was slower at late passages. MSCs cultures differently entered senescence in the course of cultivation, group I represented faster proliferating cell culture and earlier became senescent (at p5-6). Group II - slower proliferating culture and underwent senescence stage (at p8-9) (fig. 6A). We observed that MSCs senescence by typical morphological changes and cells became enlarged and flattened with enhanced SA- β -gal activity (fig. 6B). The same amount (about 30%) of SA- β -gal-positive cells was detected in first and second group at late passage p6 and p9 respectively. We analyzed molecular characteristics and

changes in mRNA expression profiles of markers, p16INK4A (p16), p21WAF1 (p21), p53, ATM (Ataxia telangiectasia mutated protein kinase) at early passage 3 of cell cultures senescence, paralleled with the monitoring of cellular morphology. As demonstrated mRNA expression analysis determined RT-qPCR, senescent AF-MSCs cultures showed increased p16 expression (fig.6C) with changes (about 14-fold vs. p3) in group I as compared with group II (about 5.5-fold vs. p3). The level of p16 expression was inversely correlated with the proliferation capability. We notice the increase in p21 and p53 expression in faster senescent cells of group I and the decrease in the level of both in slower senescent cultures at late passages from group II when compared with early passage cells. The analysis of the expression of ATM plays a role in cell cycle delay after DNA damage showed a positive correlation between increased expression levels of ATM and p53 and p21 in senescent cultures from group I and a negative from a second group. Analysis date demonstrated that MSCs cultures differently underwent cycle hold together with the decline of the efficiency of proliferation and the appearance of senescent morphology.

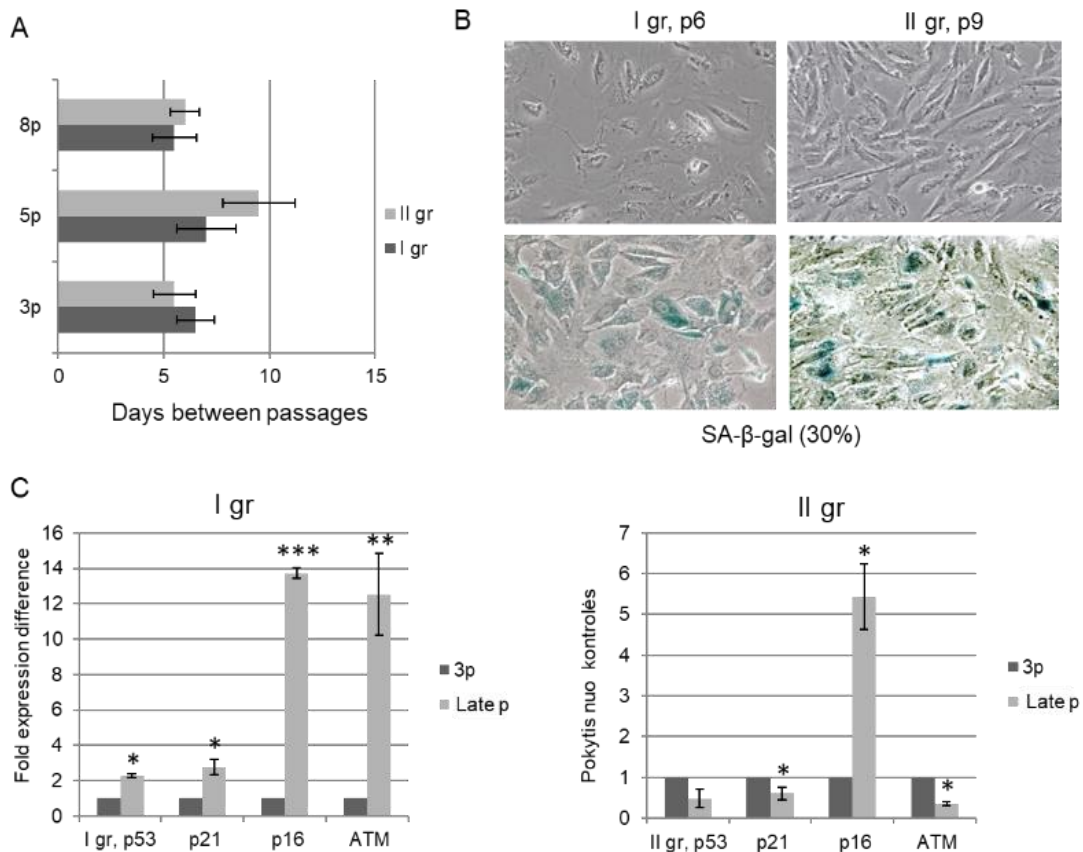


Figure 6. Characterization of senescence-associated markers in cell cultures during cultivation. (A) Differential proliferation of MSCs in two groups of cell cultures (I - II) during cultivation to passages 3, 5, 8 (n=3, for each group). (B) Non-stained (NS) and SA-β-gal positive cells at passages 6 and 9 in two groups of MSCs cultures. (C) Differential mRNA expression of senescence-associated markers in MSCs cultures (I gr and II gr) at passage 3 and the late passage was determined by RT-q-PCR. Normalization to GAPDH and fold expression difference compared with passage 3 was calculated using a comparative threshold cycle delta-delta Ct method. The data is presented as the mean ± SD (n=3, from each group). * P ≤ 0.05, ** P ≤ 0.01 and *** P ≤ 0.001 were considered as significant changes.

In order to evaluate a possible link between miRNAs and self-renewal regulating factors in senescent MSCs, we performed the comparative RT-qPCR analysis of essential transcription factors Oct4, Nanog, Sox2, Rex1 in samples of MSCs cultures from group I and group II during culturing from early passage 3 to late senescent passages. As shown (fig.7B) senescence of cells from group I caused a decrease in the expression of Oct4 and Nanog and nonsignificant changes in Sox2 and Rex1 levels. MSCs from group II showed a statistically significant decrease in expression levels of Oct4, Nanog, Sox2, and Rex1 at senescent passage compared with those at early passage 3. Likewise, miR-17 and miR21 may regulate the proliferation and senescence of MSCs through the effects on components of cell cycle machinery and possibly by the interaction with the transcription factors involved in cell proliferation and self-renewal.

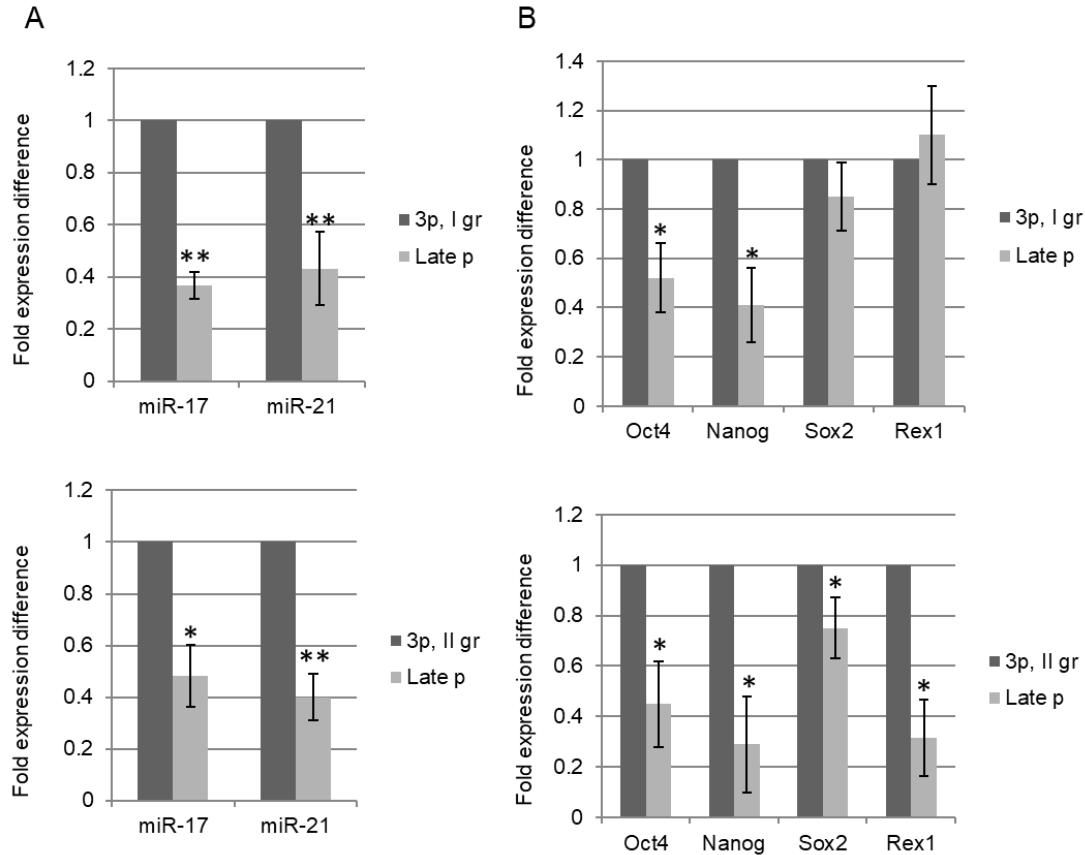


Figure 7. Differential expression of miRNAs and stem cell markers in MSCs cultures during passaging. RT-q-PCR analysis of miR-17 and miR-21 (A), and Nanog, Oct4, Sox2 and Rex1 (B) from cell cultures of two groups (I and II) at passage 3 and the late passage. Normalization to calibrator sample (A) or GAPDH (B) and fold expression difference as compared with passage 3 was calculated using a comparative threshold cycle delta-delta Ct method. The data is presented as the mean \pm SD (n=3, from each group). * $P \leq 0.05$, ** $P \leq 0.01$ and *** $P \leq 0.001$ were considered as significant changes.

3.4. Molecular and Epigenetic Alterations Associated with Senescence

We analyzed epigenetic regulatory factors as HDAC and DNMT during the cellular senescence process. The level of DNMT1 (fig. 8A) expressed in proliferating cells for the maintenance of preexisting DNA methylation, decreased in cultures of group I and II with onset of cell senescence process and became undetectable at later passage 6 in group I and at passage 8 in group II. The ATM analysis has showed

MSCs state before entering a growth arrest typical for senescence. In group I phosphorylated ATM protein (ATM-P) accumulated at passages 6 and 8 with the increase of p53, while nonphosphorylated ATM was noticed at passages 4 and 6 with the apparent decrease at late passage 8 (fig. 8B). Analysis of polycomb group proteins HDAC1, PRC2, SUZ12, EZH2, have demonstrated the expression profile similar to DNMT1, HDAC1 (fig. 8A), decrease in the levels of DNMT1 and HDAC1 at late passages occurred in all cell cultures derived from donors (D) of normal (N) and fetus-affected (P) gestation. In sample from donor D4, where MSCs senescence process was delayed, DNMT1 and HDAC1 expression were higher than in other samples at the passage 8. Protein expression changes in the levels of PRC2, SUZ12, EZH2, PRC1, component BMI1 were noticed in AF samples of the same donors, demonstrating their point in MSCs senescence process (fig. 8A and C). The inverse correlation between expression levels of histone H3K27me3 and EZH2, which specifically trimethylate histone H3 at lysine (K)27 was found in senescent cells from fetus-affected samples and were showing dynamical changes in chromatin structure. This mark accumulation occurred earlier and was maintained over passaging of faster senescent culture from sample D1. The results indicate that the epigenetic modifying enzymes, PRC1, PRC2 complex proteins and repressive histone modifications together with miRNAs cooperatively entered in senescence process of MSCs cultures derived from healthy samples and the ones with fetus-pathological gestation.

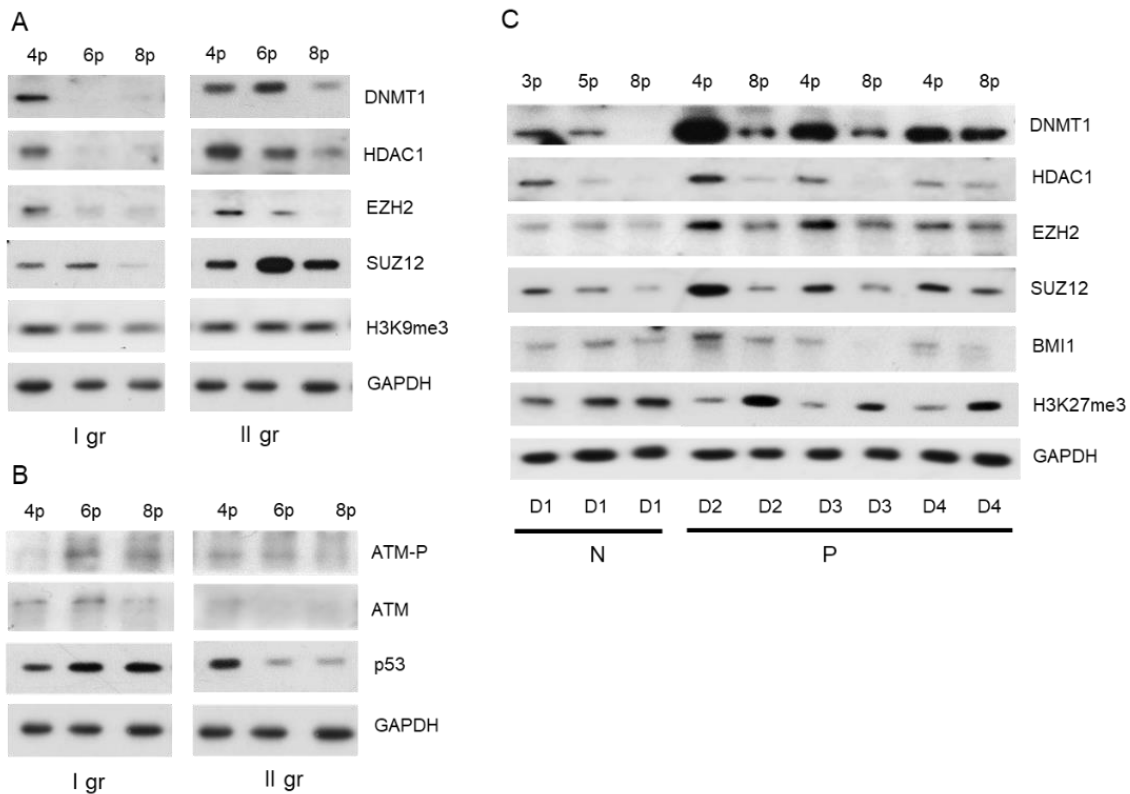


Figure 8. Epigenetic changes during passaging of cell cultures derived from AF of normal and affected gestation. Lysates from cell samples of healthy (N) donors (D) and with fetal abnormalities (P) were subjected to Western blot analysis to monitor the expression of proteins using the indicated antibodies. (A, B) Representative blots of proteins from cell cultures of two groups (I and II) during culturing at passages 4, 6 and 8, and (B) from cell cultures derived from AF of normal gestation (D1) and individual donors (D2-D4) carrying fetus abnormalities. The data is representative of at least two gels showing similar results.

3.5. AF-MSc Differentiation Potential

AF-MSCs samples from amniocenteses of different gestational time were analyzed for their capacity to differentiate to: adipogenic, osteogenic, chondrogenic, myogenic and neurogenic lineages. AF-MSCs from samples of second- (16-19 week) and third-trimester (34 week) that grew in culture from 4 or 8 passages were able to differentiate in all lineages tested (fig. 9). Cells cultured under adipogenic condition for 12 days accumulated lipid vacuoles and exhibited intense staining with Oil red (fig.9B) and performed RT-qPCR analysis showed very high expression level of adipocytes marker adiponectin that was expressed during late stages of differentiation, (456-fold increase of control) (fig. 9C). Culturing with osteogenic differentiation medium for 12 days, most of cells exhibited extracellular matrix mineralization and was detected by Alizarin red S staining and significant increase in the level of ALP. After neural culturing with specific medium, morphologically neural-like cells were observed after staining with 0.1% Crystal violet. The early morphological changes were observed after 5 days of induction and typical morphologies of neurons, such as elongated bodies, neurite-like projections and cell extensions after 12 days. Expression level of neural stem cell marker, Nestin was detected (28-fold increase relative to undifferentiated control). Myogenic differentiation and formation of myoblasts with multi-nucleated myotubes at later stages of differentiation was determined after staining with 0.1% Crystal violet (fig. 9B) and the expression of late myogenic marker Myogenin (12,3-fold increase of control) (fig. 9C). MSCs were cultured in high-density pellet mass culture for the induction of chondrogenic differentiation and it was determined after 20 days by the appearance of chondrogenic pellet and the glycosaminoglycan production was detected by Alcian blue staining. As control AF-MSCs culture has not shown any differentiation morphology (fig.9A).

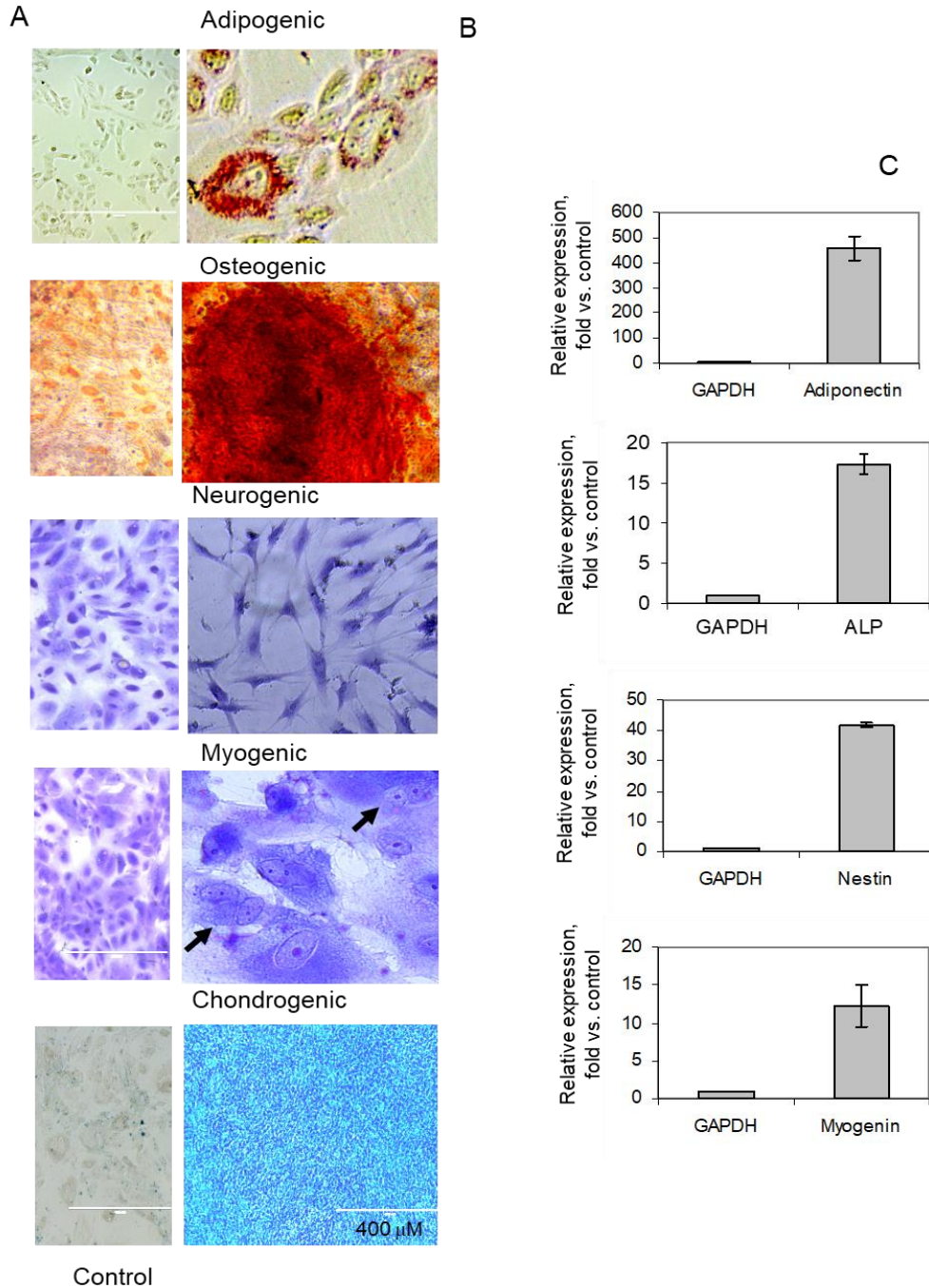


Figure 9. Differentiation potential of AF-MSCs. AF-MSCs isolated from amniocentesis samples of second- and third-trimester at passages 5-8, cultured without differentiation supplements (A) or maintained in differentiation media. (B) Representative images of AF-MSCs after adipogenic treatment showing the accumulation of lipid vacuoles by Oil Red O staining; osteogenic treatment by Alizarin Red staining for calcium mineralization; neurogenic or myogenic treatment showing the presence of neuron-like cells or multinucleated cells by staining with Crystal violet, respectively and chondrogenic treatment showing glycosaminoglycan production in chondrogenic pellets by Alcian Blue staining. (C) Relative expression of Adiponectin, Myogenin, Nestin and ALP by RT-qPCR is presented as n-fold increase over untreated control. Data are presented as the mean \pm S.N. ($p < 0.05$) for three independent experiments.

3.6. Epigenetic Alterations in AF-MSCs Cultures of Normal and Fetus-Affected Gestations

To evaluate active and repressive histone modifications in the same samples we applied immunostaining for detection of nuclear localization and antibodies against acetylated modifications of histone H4 (H4ac and H4K16ac), histone H3 (H3K14ac) and methylated modifications of histone H3 (H3K4me3, H3K9me2/me3, and H3K27me3) and stained nucleus intensities were compared. Antibodies against acetylated H4 and H3K4me3 gave positive staining but with varying intensities and patterns of localization mostly concentrated at the pericentric nuclear area (fig. 10 and 11). Repressive H3K9me2/me3 marks had predominant epigenetic distribution in the nuclei (fig. 12).

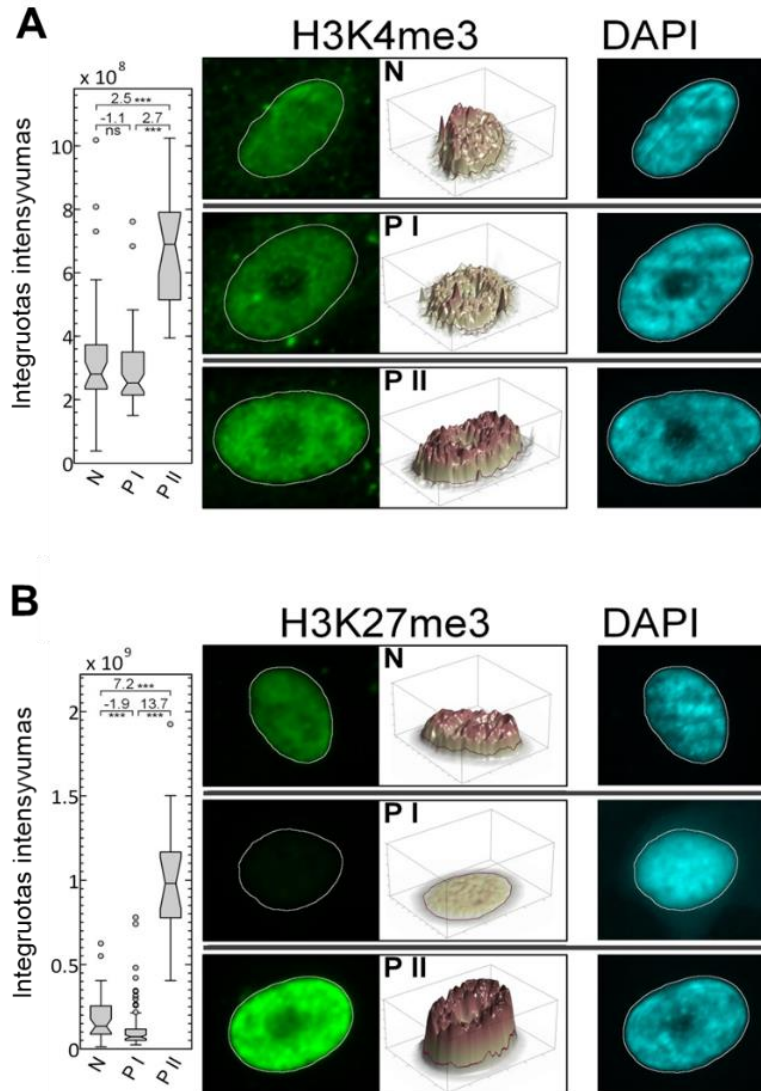


Figure 10. „Bivalent” histone modifications pattern in MSCs from AF of normal and fetus-affected gestations. Representative MSCs samples from AF of normal (donor D1) gestation and with fetal abnormalities from P I and P II cultures were immunostained with antibodies against H3K4me3 and H3K27me3. All IFIs from three experimental groups are graphed as Tukey-style box plots (left column) with sample size n=33, 56 and 22 (for H3K4me3), and n=41, 89 and 16 (for H3K27me3), respectively. Wilcoxon rank sum test was used for statistical analysis. *P<0.05, **P<0.01 and ***P<0.001 were considered as significant changes, ns - non-significant changes (P>0.05).

Immunofluorescence staining observed in MSCs for AF from normal and fetal affected pregnancies was not capable to find out differences in histone modifications pattern. The analysis of “bivalent” histone modifications (fig. 10) of PII sample indicated significantly higher levels of H3K4me3 (2.5-fold vs. N or 2.7-fold vs. PI) and H3K27me3 (7.2-fold vs. N or 12.7-fold vs. P I). Sample P I did not differ from N sample in signal intensities of H3K4me3 but it had lower level of H3K27me3 (1.9-fold of N).

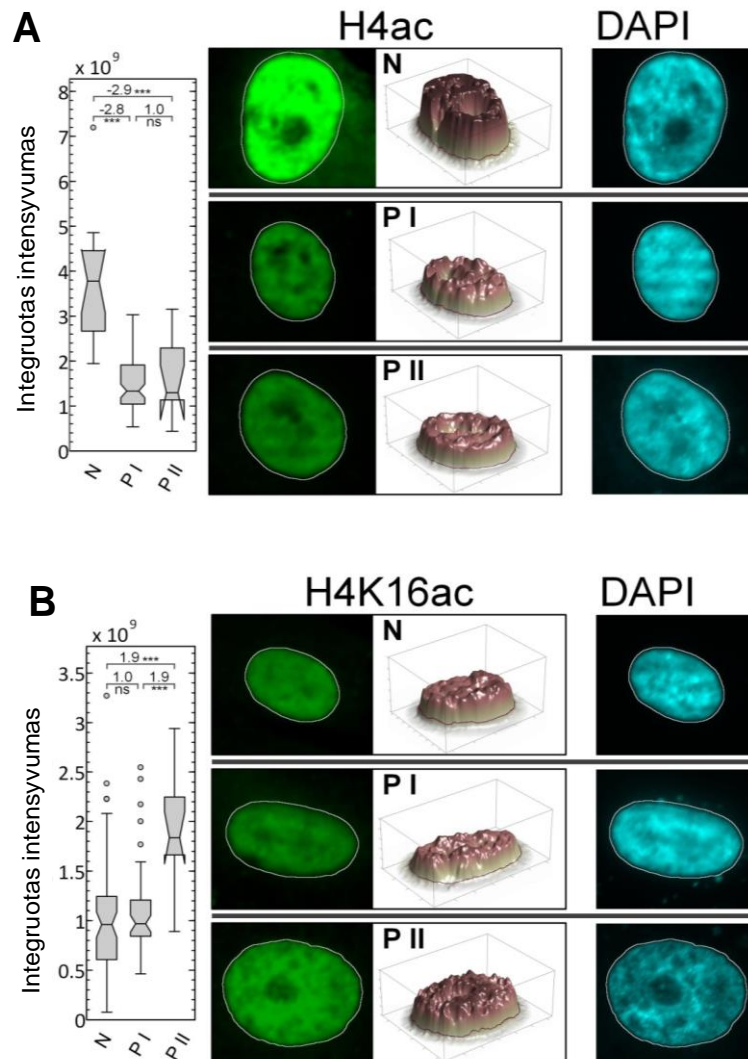


Figure 11. Changes in acetylated histone H4 modifications in MSCs of normal and fetus-affected gestations. MSCs samples from AF of D1, P I, P II cultures were immunostained with antibodies against (A) H4ac and (B) H4K16ac. Results of Alexa Fluor 488 fluorescence intensity profile are presented as conventional 2D image (middle column) and corresponding visualization as 3D surface (right column). Superimposed contours on Alexa Fluor 488 images are nuclei borders resulted from the segmentation of DAPI images (right column). Integrated fluorescent intensity (IFI) of Alexa Fluor 488 is derived by summing intensities of all the pixels that make up the nucleus region.

The level of acetylated histone H4 (fig. 11A) in N sample was 2.9-fold higher comparing with both P I and P II sample and quite similar IFIs, whereas H4K16ac mark intensity in PII sample was 1.9-fold higher than that in samples N and PI (fig. 11B). The analysis of repressive heterochromatic modifications

(fig. 12) H3K9me2/me3 in PII sample demonstrated significantly higher IFIs of both marks (1.8/5.3-fold vs. N and 7.3/3.5-fold vs. PI).

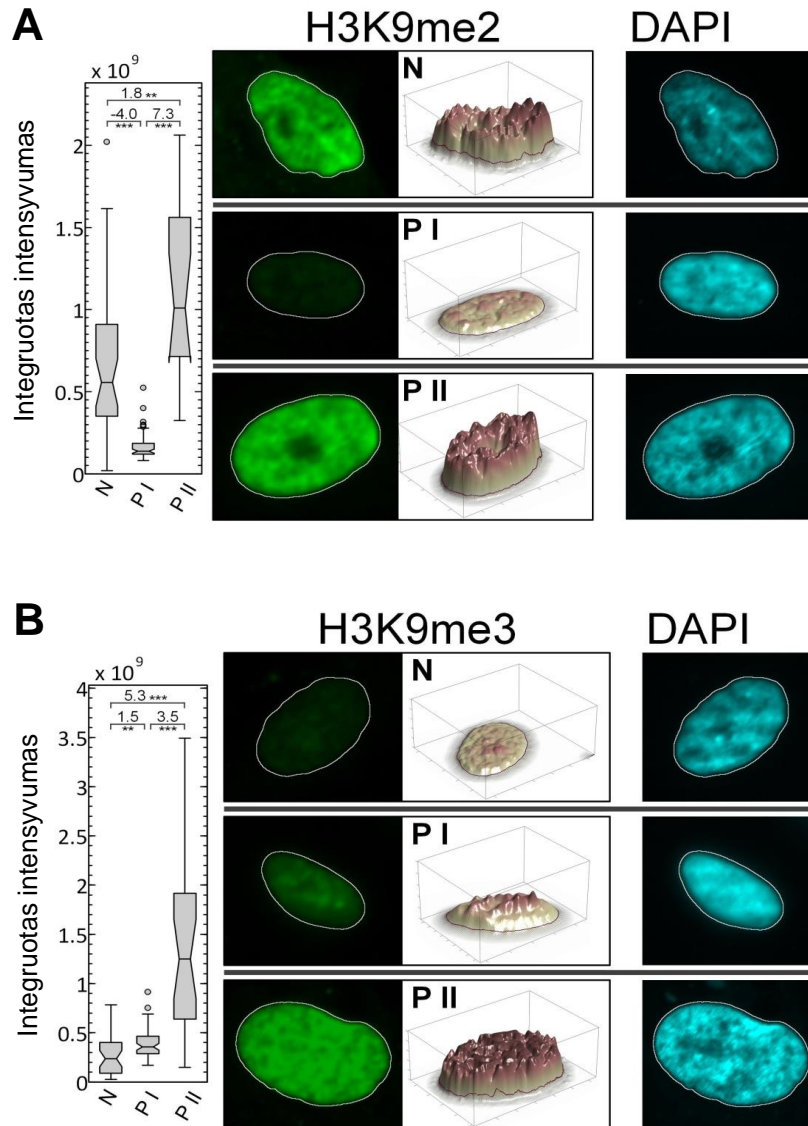


Figure 12. Changes in methylated histone H3 modifications in MSCs of normal gestation and fetus-affected gestations. Representative MSCs samples from AF of normal (donor D1) gestation and with fetal abnormalities from P I, P II cultures were immunostained with antibodies against (A) H3K9me2 and (B) H3K9me3. Results of Alexa Fluor 488 fluorescence intensity profile are presented as conventional 2D image (middle column) and corresponding visualization as 3D surface (middle right column). Superimposed contours on Alexa Fluor 488 images are nuclei borders resulted from the segmentation of DAPI images (right column). Integrated fluorescent intensity (IFI) of AlexaFluor 488 is derived by summing intensities of all the pixels that makeup the nucleus region.

Histone H3K9me2 mark was dominant in N sample culture in contrast to PI with H3K9me3 modification. Analysis shows that repressive marks and some acetylated histones (H4K16ac) clearly predominated in PII sample compared with a levels of histone modifications in PI sample. We can state the epigenetic environment was distinct in MSCs derived from AF sources dependently on the state of cell cultures or the donor individuality at conditions gestation.

3.7. Proteome Analysis of Myogenic, Adipogenic, Osteogenic, Neurogenic Differentiation in Cell Cultures

For proteome profile comparison we presented cultures of passage 5 and induced to myogenic, adipogenic, osteogenic, and neurogenic differentiation. Using SYNAPT G2 High Definition mass spectrometry based analysis resulted total of 1423 proteins expressed in AF-MSCs and proteins with the expression ratio above 1.5 compared with undifferentiated control were selected and presented. Functional classification of 250 proteins (fig. 13A) represents the selected proteins from cell cultures differentiated toward myogenic, adipogenic, osteogenic, and neurogenic lineages with the expression ratio above 1.5 vs control. The groups are: cell growth and differentiation (12%), regulation (13%), cell signaling/communication (9%), transcription/translation (8%). Other groups: represent metabolic (22%), transport (18%), structural (6%), and immune response (5%) proteins, including 7% as unknown proteins. Of 250 selected proteins (fig. 13B) 91, 89, 96, and 87 were upregulated and 89, 105, 106, and 81 down regulated in MSCs undergoing myogenic, adipogenic, osteogenic, and neurogenic differentiation respectively.

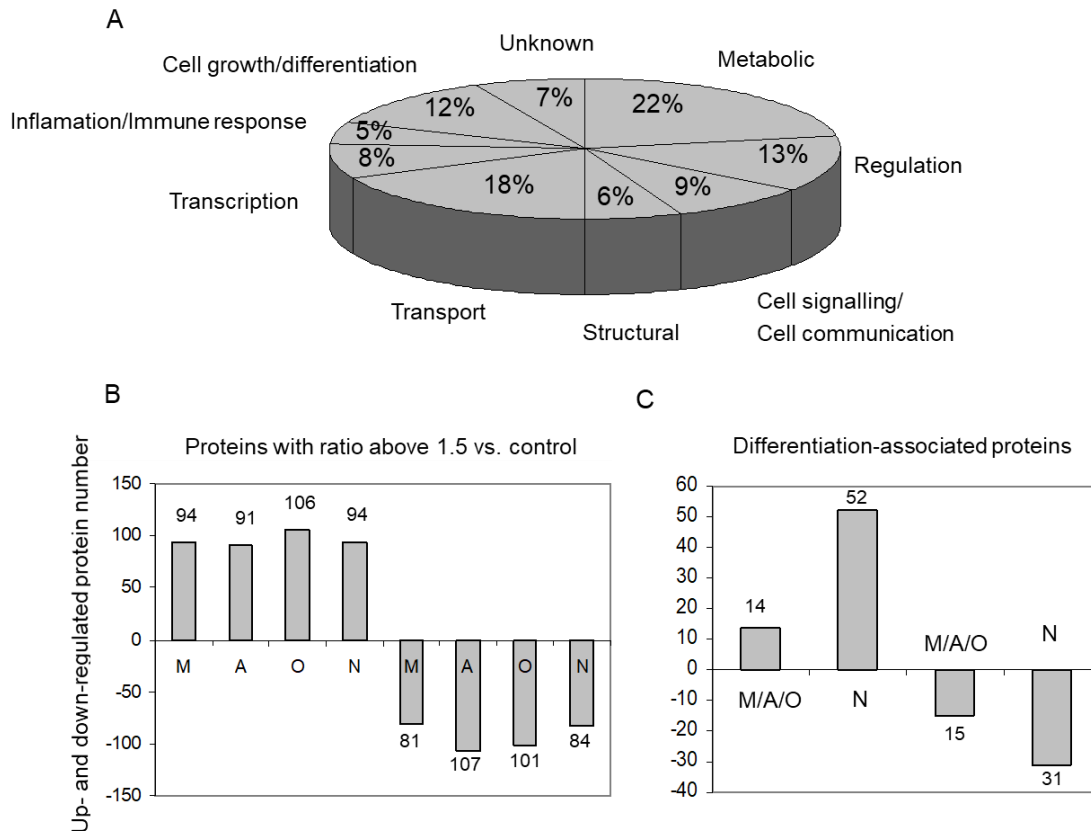


Figure 13. Differentially expressed proteins in AF-MSCs undergoing myogenic (M), adipogenic (A), osteogenic (O) and neurogenic (N) differentiation. (A) Venn diagram presents functional classification of differentiating cell proteins expressed 1.5-fold above control. (B) Number of up- and down-regulated proteins and (C) differentiation-associated proteins with ratio 1.5 vs. control in each differentiating population.

3.8. Proteins Specific for Normal and Pathological State of Pregnancies

Proteins from amniotic fluid of different state of pregnancy were isolated and fractionated in SDS/PAGE (fig.14). We separated main protein groups agreeably to molecular weight were detected: 27, 60-65 and 75-90 kDa. Quantitative level of analysed protein groups between normal vs pathological pregnancies was insignificant. All proteins were fractionated in 2DE system and visualized by staining (fig.15). In protein maps' representing normal vs effected pregnancy gestation was established more than 100 protein spots and 65 of them were identified by MALDI-TOF/TOF mass spectrometry. More than one protein was identified in one spot. By using computational methods the ratio in fold change between normal/preeclampsia AF proteins (G1/G2) and between normal/polyhydramnios (G1/G3) was evaluated. As we notice the increased levels of some proteins are common in both cases: preeclampsia and polyhydramnios and these proteins are: haptoglobin, lumican, alpha 1B glycoprotein, angiotensinogen. But some common proteins and the levels of them were decreased: transthyretin, serum amyloid P component, CD5 antigen like, hemopexin, serotransferrin, beta 2 glycoprotein 1, fibrinogen beta chain, alpha 2 macroglobulin, ceruplasmin, alpha 1 acid glycoprotein 1. The other identified proteins are more specific either for preeclampsia or polyhydramnios state of pregnancy. Only in polyhydramnios some protein levels decreased up to 2-3 fold or even 20 fold, that is haptoglobin, apolipoprotein AI, fibrinogen beta chain, clusterin.

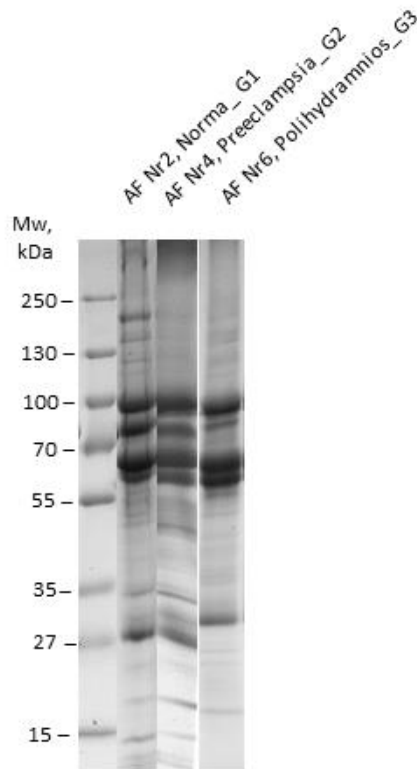


Figure 14. Amniotic fluid protein groups representing normal (G1), preeclampsia (G2) and polyhydramnios (G3) pregnancy state. Proteins were fractionated in gradient 8-18% SDS/PAGE, stained with Colloidal Coomassie G-250. Molecular weight (Mw) markers are presented on the left.

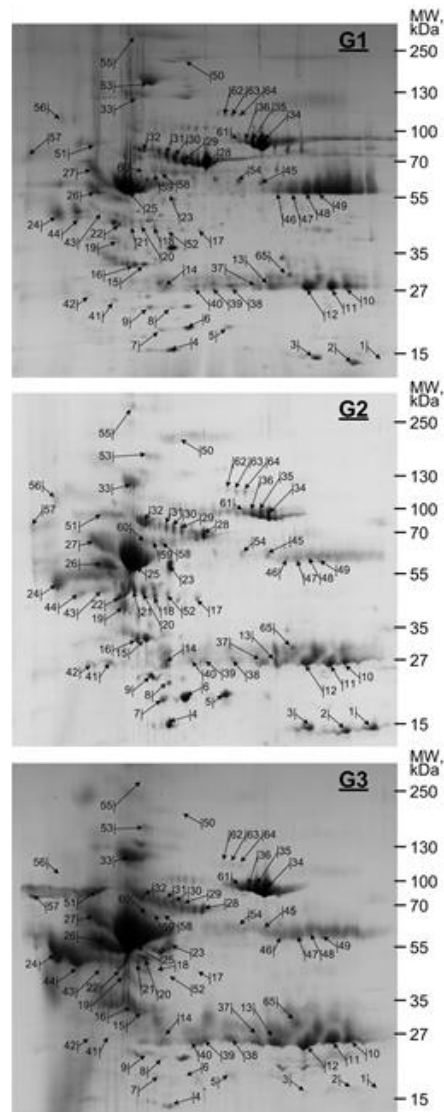


Figure 15. 2D gel electrophoretic maps of amniotic fluid proteins isolated from normal (G1), preeclampsia (G2), polyhydramnios (G3) pregnancy state. Isolated proteins were separated with 2DE and stained with Colloidal Coomassie G-250. For two-dimensional electrophoresis were used an Immobiline DryStrip Kit, pH range 3-10, and Exel Gel SDS, gradient 8-18%. Arrows and numbers in the 2DE maps indicate the positions of proteins supplied to MALDI-TOF MS/MS and identified. Representative images from one of three experiments showing similar results are shown.

3.9. Function of Proteins Specific for Normal and Pathological State of Pregnancy

By using AgBase software identified proteins in pathological pregnancies were clustered and presented (fig. 16) according to their possible function. Most of the identified proteins with increased expression in pathological state of pregnancy are cellular signaling and regulation proteins (26.5 %), pregnancy and embryo development proteins (24.5 %), metabolic proteins (15.5 %), immune response and inflammation related proteins (15.5 %) and transport proteins (9 %), transcription and structural proteins were 4.5 % and 2 % respectively. Proteins with unknown function reached volume up to 2.5 % of all analyzed proteome.

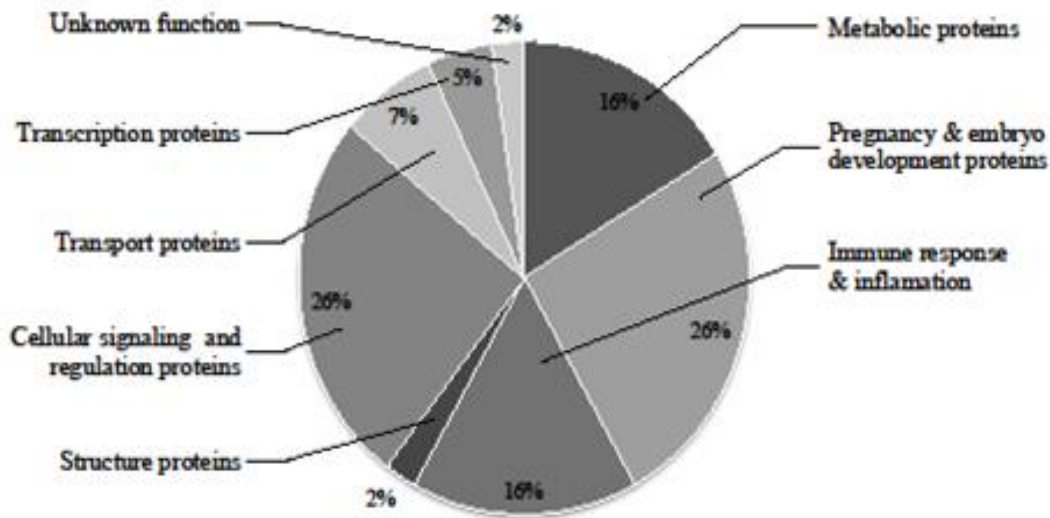


Figure 16. Functions of unique proteins of amniotic fluid with enlarged expression in pathological state of pregnancy. Proteins were clustered according their functions by using AgBase [2.00 v].

3.10. Proteomic Profile Characteristics for Normal and Polyhydramnios Amniotic Fluid

The protein profiles of amniotic fluid from normal pregnancy and of amniotic fluid from polyhydramnios pregnancy were fractionated in range pI 3-11. We analyzed 95 proteins, and only 34 proteins we detected are characteristic for AFN and AFP (pI 3-11). Most of identified proteins are increased in the amniotic fluid of polyhydramnios pregnancy. It could be mentioned ceruloplasmin, inter-alpha-trypsin inhibitor heavy chain, plasma protease C1 inhibitor, prothrombin, alpha-1B-glycoprotein, lumican, basement membrane-specific heparan sulfate proteoglycan core protein, transthyretin and others those protein spot level increased more than 2.5 times. The level of other proteins like serotransferrin in normal vs. polyhydramnios samples is changed subject to the protein spot pI, i.e. it could depend on the protein modifications. Individually the proteins characteristic for AFP were separated in 2DE with range pI 4-7 and 146 proteins were identified by mass spectrometry. In samples we identified the higher expression of some proteins and those levels were higher in comparison to proteome corresponding to normal pregnancy. Each identified protein was assigned to a certain group corresponding to protein function based on information from data agabase (www.agbase.msstate.edu) (fig. 17 and 18).

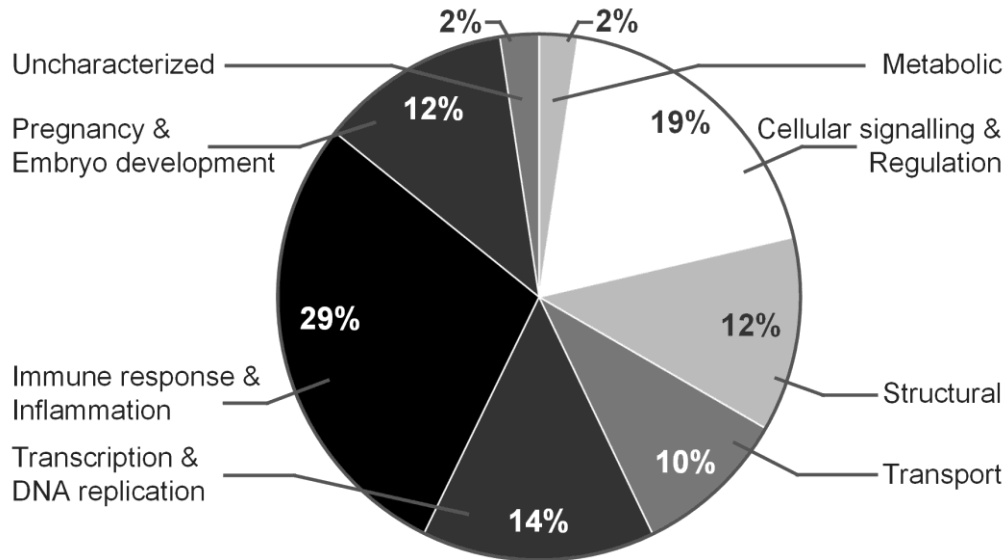


Figure 17. Functions of proteins identified in normal vs polyhydramnios pregnancies, proteins fractionated in pI 3-11 range. Proteins were clustered according their functions by using AgBase [2.00 v].

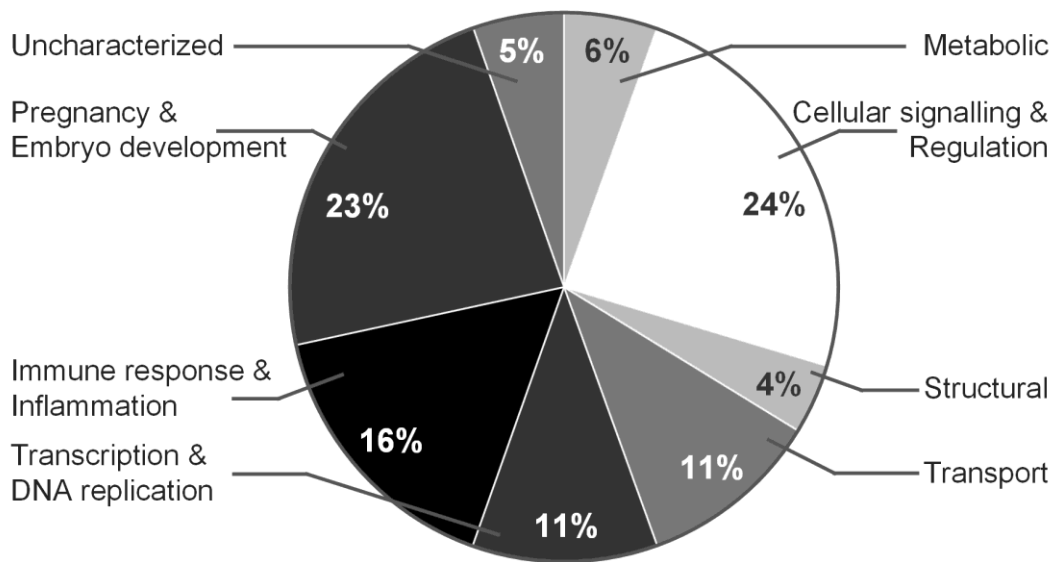


Figure 18. Functions of proteins identified in normal vs polyhydramnios pregnancies, proteins fractionated in pI 4-7 range. Proteins were clustered according their functions by using AgBase [2.00 v].

The majority of identified proteins of AFN/AFP separated in range pI 3-11 and pI 4-7 belongs to immune response and inflammation proteins – 29% (16%), cellular signalling and regulation proteins – 19% (24%), transcription and DNA replication proteins – 14% (11%), pregnancy and embryo development proteins – 12% (23%), structural proteins – 12% (4%), metabolic – 2% (6%) and involved in molecular transport system – 10% (11%). So typical amniotic fluid proteins for preeclampsia and polyhydramnios pregnancies were identified. These proteins are associated with embryo development, cell signal transduction and regulation, metabolic processes and others. Identified proteins could be important for developing new biomarkers for the detection of pathological state of pregnancy.

DISCUSSION

In our study we analyzed amniotic fluid samples from amniocentesis second-trimester (18-21 weeks of gestation) from healthy donors and donors with fetal abnormalities or/and polyhydramnios from third-trimester (29-38 weeks) isolated stem cells, AF proteins and characterized it. MSCs cultures were similar by cell morphology, immunophenotype, proliferation capability and retained the potency of differentiation to different cell lineages. But some culture cells from pathological pregnancies during passaging displayed some variations in their phenotype (CD44+, CD90+, CD105+) and proliferation potential. AF cell population, enriched with CD44+/CD105+ cells and the expression of “stemness” markers, exhibited higher proliferation rates than CD44-/CD105- population (Roubelakis et al. 2011) Its known there is evidence about exiting differences in the long-term proliferative capability of stem cells cultures and a negative correlation between donor age and MSCs proliferative capacity (Wagner et al., 2008). High expression levels of marker CD90 were found in all MCS samples, which are positive for the embryonic stem cell characteristic markers: Sox-2, Oct-4, Rex-1, Nanog that are associated with undifferentiated cell state and the pluripotency (Bossolasco et al., 2006; Kim et al., 2007). The remarks of cell growth disadvantages due to fetus abnormalities are equate with other studies, which indicated unusual growth failures related to fetal aneuploidies and gestation age (Persutte and Lenke, 1995; Moschidou et al., 2013) as well with lower growth rate in cultures of third-trimester than those of first-trimester (Shibata et al., 2007). Importantly, these cells have ability to differentiate into adipocytes, osteoblasts, chondroblasts, myocytes and neural like cells. As we observed cells from third-trimester had lower differentiation potential to myocytes and stronger to neuron-like cells and our data confirms a study (Bottai et al., 2012). Analyzing cultures we found that MSCs from second- and third trimester expressed comparable levels of factors of pluripotency and self-renewal, Nanog, Oct-4. This is consistent with the reports that cells isolated from early in pregnancy (Da Sacco et al., 2011) as well as from late mid-trimester (Dekoninck et al., 2014) expressed pluripotency markers of Oct-4 and Nanog, although decreased of Oct-4 expression (Vascotto et al., 2007). We demonstrated that cultivation of stem cells samples isolated from AF of normal and pathological pregnancies leads to senescence and is related to molecular, morphological characteristics and expressed differently in early passages, during cultivation from passage 3 to 8. Senescence associated markers of gene expression: p16, p21, p53, ATM were correlated. In faster senescent cultures p21, p53, and ATM expression notably increased but decreased in cultures with delayed senescence (fig.6). Cultures contained upper levels of senescence marker p16. Is known that cellular senescence is regulated by p53/p21 and p16/pRb pathways, where the p53/p21 pathway mediates the replicative senescence and plays important role in DNA damage response and p16/pRb pathway mediates stress-induced and premature senescence (Ben-Porath and Weinberg, 2005). So p16/pRb pathway involves and supporting a notion that p16 and p21 plays important role in initiation and maintenance of senescence (Stein et al., 1999). To date, epigenetic mechanisms and biomarkers are still undefined in human diseased gestation conditions. It's been showed in the study (Tsurubuchi et al., 2013) that in stem cell cultures from AF with neural tube defect-affected pregnancies epigenetic markers demonstrated higher levels of H3K4me2/me3 and H3K27me2/me3, and lower levels of H3K9ac and H3K18ac. And we described methylated histones H3 (at K9 and K27) and acetylated histones H3 and H4 in AF-MSCs samples from donors with diseased fetuses. We identified changes in cultures (PII) exhibiting distinct phenotypic characteristics and defective proliferation in association with a decrease in the expression of DNMT1, HDAC1, and acetylated H4 so MSCs samples were saturated with methylated histone H3 marks (H3K27me3 and H3K9me2/me3) and acetylated modifications (H4ac, H4K16ac) (figs.

10-12). It is known that methylation of H3 at K27 and K9 is associated with gene silencing, where gene repression by H3K27me3 is related to elective (developmentally regulated) heterochromatin and H3K9me2/me3 (Gan et al., 2007). Repressive (H3K9me3 and H3K27me3) histone modifications inverse to slowly growing (or senescent) samples (PII), which showed significantly higher levels of both repressive marks, H3K9me3, and H3K27me3. AF-MSCs cultures from samples with multifactorial fetal diseases displayed distinct growth and immunophenotype characteristics associated with the alterations in global DNA methylation, the pattern of acetylated histones H3, H4 and dysregulation of methylated histones H3K27 and H3K9. In this study we also focused on the specific AF proteins that could be biomarkers for fetal development and pregnancy-related disorders. Identified protein level either increased or decreased in pathological pregnancy vs. normal and are involved in various cellular processes and are responsible for cell signalling and regulation such apolipoprotein, putative elongation factor, clusterin etc., metabolic processes: lumican, vitamin D binding protein, etc., transport proteins: ceruloplasmin, etc., proteins specific for pregnancy and embryo development: angiotensinogen, fibrinogen beta chain, etc. and others. According to our results two of identified proteins specific for preeclampsia and polyhydramnios – angiotensinogen and transthyretin could be important for the prognostic marker of pathological state of pregnancy as the volume ratio of it increased from 6 to 24 times. Vascotto and co-workers (Vascotto et al., 2007) had shown that the women with preeclamptic syndrome have showed a significant increase in the amount of transthyretin monomeric proteins vs. control group. These findings coincide with our results demonstrating the increased level (up to 24.8 times) of those proteins in amniotic fluid. In pathological pregnancies we have observed some proteins that have decreased. These proteins are lumican, statherin, serotransferrin, fibrinogen, hemopexin, ceruloplasmin. All these proteins are high molecular weight and are presented in (fig.14) – the protein groups higher than 100 kDa are not detectable in preeclampsia and polyhydramnios. As these proteins lumican, serotransferrin, plasma retinol-binding protein, apolipoprotein A and others were differentially present in amniotic fluid in pregnancies with turner syndrome fetuses (Mavrou et al., 2008) as well in down syndrome (Tsangaris et al., 2011). Identified proteins: transthyretin (TTHY), α -1-microglobulin (AMBP), ceruloplasmin (CERU), afamin (AFAM), APO-E, serum amyloid P-component (SAMP), histidine-rich glycoprotein (HRG) and α -1-antitrypsin (A1AT), clusterin were upregulated in AF with pathological pregnancies. All these proteins are known to be involved in fetal growth and development and identified kinins are factors for the biological activity of the amniotic fluid (Choolani et al., 2009). Proteins were identified that are typical for amniotic fluid of preeclampsia and polyhydramnios pregnancies and these proteins are associated with embryo development, cell signal transduction, regulation, metabolic processes and others. Identified proteins angiotensinogen, transthyretin, transferrin, lumican, serotransferin and others could be important for developing and detection of pathological state of pregnancy. These proteins with significantly variable expression levels in amniotic fluid of normal and pathological pregnancy state could become valuable biomarkers.

Amniotic fluid stem cells are unique because of their ability to differentiate into different types of cells and form a broad array of cells and tissue. Their multipotency is an important advantage relative to adult organism-derived stem cells those mostly can differentiate into one type of cells.

CONCLUSIONS

1. AF-MSCs, isolated from amniotic fluid of second and third trimester of pregnancies, present immunophenotypic characteristics and stemness markers (*CD44*, *CD90*, *CD105*, *Sox2*, *Rex1*, *Nanog*, *Oct4*) and their proliferation potential vary depending on the individual, gestation age and pregnancy pathology.
2. Aging of AF-MSCs are determined by morphological and epigenetic changes as well as the expression of aging-related protein markers (*p16*, *p21*, *p53*, *ATM*), microRNA (*miR-17*, *miR-21*) – their expression depends on the aging process intensity.
3. AF-MSCs from normal and pathological pregnancies represent an active profile of histone modifications (*H4ac*, *H4K16ac*, *H3K4me3*, *etc.*) and repressive histone modifications (*H3K9me2/3*, *H3K27me3*), depending on their phenotypic and growth characteristics.
4. By using detail proteomic analysis we identified specific proteins and their changes related to specific differentiation – *TMOD2*, *K1C9*, *K1C14*, *K1C16*, and *K2C14* for myogenic differentiation; *GPNMB*, *S10A4* for osteogenic differentiation; *PTK7*, *GPNB*, *ITA8*, and *WNT5A* for neurogenic differentiation.
5. We have identified protein level differences in amniotic fluid samples characteristic for pathological pregnancies with preeclampsia and polyhydramnios vs normal pregnancy. In increased protein level in pathological pregnancies were determined – *transthyretin*, *angiotensinogen*. In decreased protein level – *lumican*, *hemopexin*, *serotransferrin*, *fibrinogen*.

REFERENCES

1. Antonucci I, Stuppia L, Kaneko Y, Yu S, Tajiri N, Bae EC, *et al.* Amniotic fluid as a rich source of mesenchymal stromal cells for transplantation therapy. *Cell Transplant.* 2011; 20(6):789–795.
2. Ben-Porath I, Weinberg RA. The signals and pathways activating cellular senescence. *Int J Biochem Cell Biol.* 2005; 37(5):961–976.
3. Bossolasco P, Montemurro T, Cova L, Zangrossi S, Calzarossa C, Buiatitotis S. Molecular and phenotypic characterization of human amniotic fluid cells and their differentiation potential. *Cell Res.* 2006; 16:329–336.
4. Bottai D, Cigognini D, Nicoraetal E. Third trimester amniotic fluid cells with the capacity to develop neural phenotypes and with heterogeneity among sub-populations. *Restor Neurol Neurosci.* 2012; 30(1):55–68.
5. Choolani M, Narasimhan K, Kolla V, Hahn S. Proteomic Technologies for Prenatal Diagnostics: Advances and Challenges Ahead. *Expert Rev Proteomics.* 2009; 87–101.
6. Da Sacco S, De Filippo RE, Perin L. Amniotic fluid as a source of pluripotent and multipotent stem cells for organ regeneration. *Curr Opin Organ Transplant.* 2011; 16(1):101–105.
7. Dekoninck P, Toelen J, Zia S. Routine isolation and expansion late mid trimester amniotic fluid derived mesenchymal stem cells in a cohort of fetuses with congenital diaphragmatic hernia. *European Journal of Obstetrics Gynecology and Reproductive Biology,* 2014; 178, 157–162.
8. Gan Q, Yoshida T, McDonald OG, Owens GK. Concise review: Epigenetic mechanisms contribute to pluripotency and cell lineage determination of embryonic stem cells. *Stem Cells.* 2007; 25:2–9.
9. Hamid AA, Joharry MK, Mun-Fun H, Hamzah SN, Rejali Z, Yazid MN, *et al.* Highly potent stem cells from full-term amniotic fluid: a realistic perspective. *Reprod Biol.* 2017; 17(1):9–18.
10. Ivanovs A, Rybtstov S, Anderson RA, Turner ML, Medvinsky A. Identification of the niche and phenotype of the first human hematopoietic stem cells. *Stem Cell Reports.* 2014; 2(4):449–456.
11. Kim J, Lee Y, Kim H, Hwang KJ, Kwon HC, Kim SK, *et al.* Human amniotic fluid-derived stem cells have characteristics of multipotent stem cells. *Cell Prolif.* 2007; 40(1):75–90.
12. Mavrou A, Anagnostopoulos AK, Kolialexi A, Vougas K, Papantoniou N, Antsaklis A, *et al.* Proteomic analysis of amniotic fluid in pregnancies with Turner syndrome fetuses. *J. Proteome Res.* 2008; 7(5):1862–1866.
13. Mohamed-Ahmed S, Fristad I, Lie SA, Suliman S, Mustafa K, Vindenes H, *et al.* Adipose-derived and bone marrow mesenchymal stem cells: a donor-matched comparison. *Stem Cell Res Ther.* 2018; 9(1):168.
14. Moschidou D, Drews K, Eddaoudi AJ, De Coppi P, Guillot PV. Molecular signature of human amniotic fluid stem cells during fetal development. *Curr Stem Cell Res Ther.* 2013; 8:73–81.
15. Persutte WH, Lenke RR. Failure of amniotic-fluid-cell growth: is it related to fetal aneuploidy? *Lancet.* 1995; 345(8942):96–97.
16. Prusa AR, Marton E, Rosner M, Bernaschek G, Hengstschlager M. Oct-4-expressing cells in human amniotic fluid: a new source for stem cell research? *Hum Reprod.* 2003; 18(7):1489–1493.
17. Roubelakis MG, Bitsika V, Zagoura D, Trohatou O, Pappa KI, Makridakis M, *et al.* In vitro and in vivo properties of distinct populations of amniotic fluid mesenchymal progenitor cells. *J Cell Mol Med.* 2011; 15(9):1896–1913.

18. Roubelakis MG, Trohatou O, Anagnostou NP. Amniotic fluid and amniotic membrane stem cells: marker discovery. *Stem Cells Int.* 2012; Article ID 107836, 9 pages.
19. Savickiene J, Treigyte G, Baronaite S, Valiuliene G, Kaupinis A, Valius M, *et al.* Human Amniotic Fluid Mesenchymal Stem Cells from Second- and Third-Trimester Amniocentesis: Differentiation Potential, Molecular Signature, and Proteome Analysis. *Stem Cells Int.* 2015, Article ID 319238, 15 pages.
20. Shibata KR, Aoyama T, Shima Y, Fukiage K, Otsuka S, Furu M, *et al.* Expression of the p16INK4A gene is associated closely with senescence of human mesenchymal stem cells and is potentially silenced by DNA methylation during in vitro expansion. *Stem Cells.* 2007; 25(9):2371–2382.
21. Stein GH, Drullinger LF, Soulard A, Dulic V. Differential roles for cyclin-dependent kinase inhibitors p21 and p16 in the mechanisms of senescence and differentiation in human fibroblasts. *Mol Cell Biol.* 1999; 19(3):2109–2117.
22. Stolzing A, Jones E, McGonagle D, Scutt A. Age-related changes in human bone marrow-derived mesenchymal stem cells: consequences for cell therapies. *Mech Ageing Dev.* 2008; 129(3):163–173.
23. Tsangaris GT, Anagnostopoulos AK, Tounta G, Antsaklis A, Mavrou A, Kolialexi A. Application of proteomics for the identification of biomarkers in amniotic fluid: are we ready to provide a reliable prediction? *EPMA J.* 2011; 2(2):149–155.
24. Vascotto C, Salzano AM, D'Ambrosio C, Fruscalzo A, Marchesoni D, di Loreto C, *et al.* Oxidized transthyretin in amniotic fluid as an early marker of preeclampsia. *J Proteome Res.* 2007; 6(1):160–170.
25. Wagner W, Horn P, Castoldi M, Diehlmann A, Bork S, Saffrich R, *et al.* Replicative senescence of mesenchymal stem cells: a continuous and organized process. *PLoS One.* 2008; 3(5): e2213.

PUBLICATIONS

1. Savickiene J, Treigyte G, **Baronaite S**, Valiulienė G, Kaupinis A, Valius M, Arlauskienė A, Navakauskienė R. Human Amniotic Fluid Mesenchymal Stem Cells from Second- and Third-Trimester Amniocentesis: Differentiation Potential, Molecular Signature, and Proteome Analysis. *Stem Cells International*. 2015, 2015:319238.
2. Navakauskienė R, **Baronaite S**, Matuzevicius D, Zaikova I, Arlauskienė A, Navakauskas D, Treigyte G. Identification and Characterization of Amniotic Fluid Proteins Incident to Normal, Preeclampsia and Polyhydramnios Pregnancies. *Current Proteomics*. 2016, 13 (3):206-217.
3. Savickienė J, **Baronaitė S**, Zentelytė A, Treigyte G, Navakauskienė R. Senescence-Associated Molecular and Epigenetic Alterations in Mesenchymal Stem Cell Cultures From Amniotic Fluid of Normal and Fetus-Affected Pregnancy. *Stem Cells International*. 2016, 2016:2019498.
4. Savickienė J, Matuzevičius D, **Baronaitė S**, Treigyte G, Krasovskaja N, Zaikova I, Navakauskas D, Utkus A, Navakauskienė R. Histone Modifications Pattern Associated With a State of Mesenchymal Stem Cell Cultures Derived From Amniotic Fluid of Normal and Fetus-Affected Gestations. *Journal of Cellular Biochemistry*. 2017, 118(11):3744-3755.
5. **Baronaite S**, Matuzevicius D, Treigyte G, Arlauskienė A, Serackis A, Navakauskas D, Navakauskienė R. Proteomic characterization of amniotic fluid in polyhydramnios pregnancies – a direct computational analysis tool for prenatal medicine. 2018.

ACKNOWLEDGEMENTS

Successful and interesting writing of the dissertation would not be implemented without the work of the head of staff, colleagues - the employees of the Department of Molecular Cell Biology, the researchers of the Proteomics Center and the VULSK doctors.

In particular, I would like to thank:

To my scientific supervisor prof. Rūta Navakauskienė for the development of work ideas, support, advice and training, very comprehensive and creative leadership at all stages of scientific work.

Clinical consultant gynaecologist doc. Audronė Arlauskienė for interpretations of clinical cases, as well as professional cooperation in the analysis of biological samples.

Gynaecologist-geneticist Natalia Krasovskaja for the possibility to obtain important biological samples by amniocentesis.

Dr. Gražina Treigyte and dr. Jūratė Savickienė for a practical and theoretical experience, advices.

PhD student Aistė Zentelytė for the contribution to perform flow cytometry and RT-qPCR analysis.

Curriculum vitae

Personal information

Sandra Baronaitė

baronaite.sandra@gmail.com; Phone number +37061619700

Education

2011 - 2017 PhD student, Department of Molecular Cell Biology, Institute of Biochemistry, Life Sciences Center, Vilnius University, Vilnius, Lithuania.

2007 – 2009 Master in chemistry, Vilnius Educological University, Studentų st. 39, LT-08106 Vilnius, Lithuania.

1999 – 2007 Bachelor in chemistry, Vilnius Educological University, Studentų st. 39, LT-08106 Vilnius, Lithuania.

Work experience

2015 – 2017 Junior research associate/researcher, Institute of Biochemistry, Vilnius University.

Participation in scientific project

The role of epigenetic factors and microRNA in amniotic fluid derived stem cells functioning, Contract No. MIP-57/2015. Participant of the project.

The role of molecular modulators in the hematological system during cell senescence, differentiation and regeneration, Contract No. LIG-12/2015. Participant of the project.

Cytological, molecular and epigenetic studies of amniotic fluid, Contract No. MIP-033/2013. Participant of the project.

Multiplexed molecular biomarker study for leukemia, Contract No. LIG-06/2012. Participant of the project.

Scientific interest

Stem cells, molecular biology, prenatal diagnostics, embryology, regenerative medicine.

Vilniaus universiteto leidykla
Universiteto g. 1, LT-01513 Vilnius
El. p. info@leidykla.vu.lt,
www.leidykla.vu.lt
Tiražas 30 egz.